PHYSICAL REVIEW D **80,** 035021 (2009)

Probing new physics in charm couplings with flavor-changing neutral currents

Xiao-Gang He* and Jusak Tandean†

Department of Physics and Center for Theoretical Sciences, National Taiwan University, Taipei 106, Taiwan

G. Valencia‡

Department of Physics and Astronomy, Iowa State University, Ames, Iowa 50011, USA

(Received 27 April 2009; published 25 August 2009)

Low-energy experiments involving kaon, B-meson, D-meson, and hyperon flavor-changing neutral transitions have confirmed the loop-induced flavor-changing neutral current picture of the standard model. The continuing study of these processes is essential to further refine this picture and ultimately understand the flavor dynamics. In this paper we consider deviations from the standard model in the charm sector and their effect on flavor-changing neutral current processes. Specifically, we parametrize new physics in terms of left- and right-handed anomalous couplings of the W boson to the charm quark. We present a comprehensive study of existing constraints and point out those measurements that are most sensitive to new physics of this type.

DOI: 10.1103/PhysRevD.80.035021 PACS numbers: 12.60.Cn, 12.15.Lk, 12.38.Bx, 13.20.−v

I. INTRODUCTION

One of the outstanding problems for high-energy physics remains the understanding of the dynamics of flavor. Existing experimental results on kaon, D-meson, B-meson, and hyperon decays, as well as neutral-meson mixing, are all consistent with the loop-induced nature of flavor-changing neutral currents (FCNC's) in the standard model (SM) and also with the unitarity of the Cabibbo-Kobayashi-Maskawa (CKM) matrix with three generations. The continuing study of these processes with increased precision will play a crucial role in the search for physics beyond the SM.

In many types of new physics, the new particles are heavier than their SM counterparts and their effects can be described by an effective low-energy theory. A complete set of operators of dimension six describing deviations from the SM has been presented in Ref. [1]. A less ambitious program is to study only those operators that appear when the new physics effectively modifies the SM couplings between gauge bosons and certain fermions [2]. The case of anomalous top-quark couplings has been treated before in the literature [3,4], and it was found that they are most tightly constrained by the $b \to s\gamma$ decay. Interestingly, this mode does not place severe constraints on anomalous charm-quark couplings due to the relative smallness of the charm mass.

In this paper we focus on new physics affecting primarily the charged weak currents involving the charm quark. Including the SM term, the effective Lagrangian in the unitary gauge for a general parametrization of anomalous interactions of the W boson with an up-type quark U_k and a down-type quark D_l can be written as

$$\mathcal{L}_{UDW} = -\frac{g}{\sqrt{2}} V_{kl} \bar{U}_k \gamma^\mu [(1 + \kappa_{kl}^{\mathrm{L}}) P_{\mathrm{L}} + \kappa_{kl}^{\mathrm{R}} P_{\mathrm{R}}] D_l W_\mu^+ + \mathrm{H.c.}, \quad (1)$$

where g is the weak coupling constant, we have normalized the anomalous couplings $\kappa_{kl}^{\mathrm{L,R}}$ relative to the usual CKM-matrix elements V_{kl}, and $P_{\mathrm{L,R}} = \frac{1}{2}(1 \mp \gamma_5)$. In general, $\kappa_{kl}^{\mathrm{L,R}}$ are complex and, as such, provide new sources of CP violation. In Appendix A we discuss the general parametrization of the quark-mixing matrix underlying Eq. (1), paying particular attention to the number of independent parameters that are allowed.

In addition to affecting weak decays though tree-level interactions, the new couplings in Eq. (1) modify effective flavor-changing and -conserving couplings at one loop. In this work, we evaluate several one-loop transitions induced by the new couplings via magnetic-dipole, penguin, and box diagrams. We include the operators generated this way in our phenomenological analysis.

We present a comprehensive picture of existing constraints which shows that deviations from SM couplings at the percent level are still possible, particularly for right-handed interactions. Our study will also serve as a guide as to which future measurements provide the most sensitive tests for new physics that can be parametrized with anomalous W-boson couplings to the charm quark. For the CP-violating (imaginary) parts of the couplings, the electric dipole moment of the neutron and the hyperon asymmetry $A_{\Xi\Lambda}$ are the most promising channels to probe for right-handed couplings, whereas more precise measurements of $\sin(2\beta)$ and $\sin(2\beta_s)$ are the most promising probes for left-handed couplings. Constraints on the real parts of the right-handed couplings can be further improved with better measurements of semileptonic B and D decays.

*hexg@phys.ntu.edu.tw
†jtandean@yahoo.com
‡valencia@iastate.edu

II. ONE-LOOP PROCESSES

In this section, we collect the main formulas for the loop-induced processes we are considering. All our calculations are performed in the unitary gauge, and the results have been compared to existing ones, where available. We have summarized our loop calculations in Appendix B.

A. Dipole penguin operators

Of particular interest are the electromagnetic and chromomagnetic dipole operators, which can give rise to potentially large corrections to SM processes [5,6] and be expressed as

$$Q_\gamma^\pm = \frac{e}{16\pi^2}(\bar{d}'\sigma_{\mu\nu}P_R d \pm \bar{d}'\sigma_{\mu\nu}P_L d)F^{\mu\nu}, \tag{2}$$

$$Q_g^\pm = \frac{g_s}{16\pi^2}(\bar{d}'\sigma_{\mu\nu}t_a P_R d \pm \bar{d}'\sigma_{\mu\nu}t_a P_L d)G_a^{\mu\nu}, \tag{3}$$

where d and $d' \neq d$ are down-type quarks, $F^{\mu\nu}$ and $G_a^{\mu\nu}$ are the usual photon and gluon field-strength tensors, respectively, with e and g_s being their coupling constants, and $\mathrm{Tr}(t_a t_b) = \frac{1}{2}\delta_{ab}$. The main effect of these operators is generated at one loop with the W boson coupling to the left-handed current at one vertex and to the right-handed current at the other vertex. It corresponds to the terms linear in the κ^R's in Eqs. (B1) and (B2), leading to the effective Hamiltonian

$$\mathcal{H}_{\gamma,g} = C_\gamma^+ Q_\gamma^+ + C_\gamma^- Q_\gamma^- + C_g^+ Q_g^+ + C_g^- Q_g^- + \mathrm{H.c.}, \tag{4}$$

where at the W-mass scale

$$C_\gamma^\pm(m_W) = -\sqrt{2}G_F \sum_{q=u,c,t} V_{qd'}^* V_{qd}(\kappa_{qd}^R \pm \kappa_{qd'}^{R*}) m_q F_0(x_q),$$
$$C_g^\pm(m_W) = -\sqrt{2}G_F \sum_{q=u,c,t} V_{qd'}^* V_{qd}(\kappa_{qd}^R \pm \kappa_{qd'}^{R*}) m_q G_0(x_q), \tag{5}$$

with G_F being the Fermi constant, $x_q = \bar{m}_q^2(m_q)/m_W^2$, and F_0 and G_0 given in Eqs. (B6) and (B7). The contributions of these operators are potentially enlarged relative to the corresponding ones in the SM due to the enhancement factors of m_c/m_s and m_t/m_b in $s \to d$ and $b \to (d, s)$ transitions, respectively, and also due to $F_0(x_q)$ and $G_0(x_q)$ being larger than their SM counterparts. For the case of anomalous tbW couplings, the formulas above agree with those found in the literature [3].

B. Electric dipole moments

The flavor-conserving counterparts of $Q_{\gamma,g}$ above contribute to the electric and color dipole-moments of the d and s quarks. Based on Eqs. (4) and (5), one can write the effective Hamiltonian for such contributions to the dipole moments of the d quark as

$$\mathcal{H}_d^{\mathrm{dm}} = \frac{i}{2} d_d^{\mathrm{edm}} \bar{d}\sigma_{\mu\nu}\gamma_5 d F^{\mu\nu} + \frac{i}{2} d_d^{\mathrm{cdm}} \bar{d}\sigma_{\mu\nu} t_a \gamma_5 d G_a^{\mu\nu}, \tag{6}$$

where in our case

$$d_d^{\mathrm{edm}}(m_W) = \frac{-eG_F}{2\sqrt{2}\pi^2} \sum_{q=u,c,t} |V_{qd}|^2 \,\mathrm{Im}\kappa_{qd}^R m_q F_0(x_q),$$
$$d_d^{\mathrm{cdm}}(m_W) = \frac{-g_s G_F}{2\sqrt{2}\pi^2} \sum_{q=u,c,t} |V_{qd}|^2 \,\mathrm{Im}\kappa_{qd}^R m_q G_0(x_q) \tag{7}$$

at the m_W scale. These expressions agree with those derived from quark-W loop diagrams in a left-right model [7], after appropriate changes are made. The corresponding quantities for the s quark are similar in form. Since the dipole moments $d_{d,s}$ contribute to the electric dipole moment of the neutron [8–10], it can be used to place constraints on $\mathrm{Im}\kappa_{qd,qs}^R$.

C. Operators generated by Z-penguin, γ-penguin, and box diagrams

The anomalous quark-W couplings also generate flavor-changing neutral-current interactions via Z-penguin, γ-penguin, and box diagrams. They will therefore affect other loop-generated processes, such as $K \to \pi\nu\bar{\nu}$, $K_L \to \ell^+\ell^-$, and neutral-meson mixing.

The effective theory with anomalous couplings is not renormalizable, and this results in divergent contributions to some of the processes we consider. These divergences are understood in the context of effective field theories as contributions to the coefficients of higher-dimension operators. These operators then enter the calculation as additional "anomalous couplings," introducing new parameters to be extracted from experiment. For our numerical analysis, we will limit ourselves to the anomalous couplings of Eq. (1), ignoring the higher-dimension operators. In so doing, we trade the possibility of obtaining precise predictions in specific models for order-of-magnitude estimates of the effects of new physics parametrized in a model-independent way. We will rely on the common procedure [11] of using dimensional regularization, dropping the resulting pole in four dimensions, and identifying the renormalization scale μ with the scale of the new physics underlying the effective theory. Our results will thus contain a logarithmic term of the form $\ln(\mu/m_W)$ in which we set $\mu = \Lambda = 1$ TeV for definiteness. In addition to the logarithmic term representing the new-physics contribution, we have also kept in our estimates those finite terms that correspond to contributions from SM quarks in the loops.[1]

[1]Explicit examples of the type of divergence cancellation resulting in a logarithmic term as described above can be found in Ref. [12], where the new-physics scale is given by the masses of non-SM Higgs-bosons.

We consider the contributions of the anomalous couplings to $d\bar{d}' \to \nu\bar{\nu}$, $d\bar{d}' \to \ell^+\ell^-$, and $d\bar{d}' \to \bar{d}d'$, relegating the main results of the calculation to Appendix B. It follows that the effective Hamiltonians generated by the anomalous charm couplings are at the m_W scale

$$\mathcal{H}^{\kappa}_{d\bar{d}'\to\nu\bar{\nu}} = \frac{\alpha G_F \lambda_c(\kappa^L_{cd} + \kappa^{L*}_{cd'})}{\sqrt{8}\pi \sin^2\theta_W}\left(-3\ln\frac{\Lambda}{m_W} + 4X_0(x_c)\right)\bar{d}'\gamma^\sigma P_L d\bar{\nu}\gamma_\sigma P_L \nu + \frac{\alpha G_F \lambda_c \kappa^R_{cd}\kappa^{R*}_{cd'}}{\sqrt{8}\pi \sin^2\theta_W}\left[(4x_c - 3)\ln\frac{\Lambda}{m_W} + \tilde{X}(x_c)\right]\bar{d}'\gamma^\sigma P_R d\bar{\nu}\gamma_\sigma P_L \nu, \tag{8}$$

$$\mathcal{H}^{\kappa}_{d\bar{d}'\to\ell^+\ell^-} = \frac{\alpha G_F \lambda_c(\kappa^L_{cd} + \kappa^{L*}_{cd'})}{\sqrt{8}\pi}\left[\left(3\ln\frac{\Lambda}{m_W} - 4Y_0(x_c)\right)\frac{\bar{d}'\gamma^\sigma P_L d\bar{\ell}\gamma_\sigma P_L \ell}{\sin^2\theta_W} + \left(-\frac{16}{3}\ln\frac{\Lambda}{m_W} + 8Z_0(x_c)\right)\bar{d}'\gamma^\sigma P_L d\bar{\ell}\gamma_\sigma \ell\right] + \frac{\alpha G_F \lambda_c \kappa^R_{cd}\kappa^{R*}_{cd'}}{\sqrt{8}\pi}\left\{\left[(3 - 4x_c)\ln\frac{\Lambda}{m_W} + \tilde{Y}(x_c)\right]\frac{\bar{d}'\gamma^\sigma P_R d\bar{\ell}\gamma_\sigma P_L \ell}{\sin^2\theta_W} + \left[\left(8x_c - \frac{16}{3}\right)\ln\frac{\Lambda}{m_W} + \tilde{Z}(x_c)\right]\bar{d}'\gamma^\sigma P_R d\bar{\ell}\gamma_\sigma \ell\right\}, \tag{9}$$

$$\mathcal{H}^{\kappa}_{d\bar{d}'\to\bar{d}d'} = \frac{G_F^2 m_W^2}{8\pi^2}\lambda_c(\kappa^L_{cd} + \kappa^{L*}_{cd'})\left(-\lambda_t x_t \ln\frac{\mu^2}{m_W^2} - \sum_q \lambda_q \mathcal{B}_1(x_q, x_c)\right)\bar{d}'\gamma^\alpha P_L d\bar{d}'\gamma_\alpha P_L d + \frac{G_F^2 m_W^2}{4\pi^2}\lambda_c \kappa^R_{cd}\kappa^{R*}_{cd'}\left(-\lambda_t x_t \ln\frac{\mu^2}{m_W^2} - \sum_q \lambda_q \mathcal{B}_2(x_q, x_c)\right)\bar{d}'\gamma^\alpha P_L d\bar{d}'\gamma_\alpha P_R d + \frac{G_F^2 m_W^2}{4\pi^2}\lambda_c^2 x_c\left(-\ln\frac{\mu^2}{m_W^2} - \mathcal{B}_3(x_c, x_c)\right)[(\kappa^R_{cd})^2\bar{d}'P_R d\bar{d}'P_R d + (\kappa^{R*}_{cd'})^2\bar{d}'P_L d\bar{d}'P_L d] \tag{10}$$

where $d' \neq d$, we have kept terms linear in κ^L and quadratic in κ^R, $\lambda_q = V^*_{qd'}V_{qd}$, and θ_W is the Weinberg angle. The functions X_0, Y_0, Z_0, $\tilde{X}$, $\tilde{Y}$, $\tilde{Z}$, and $\mathcal{B}_{1,2,3}$ can be found in Appendix B.

III. TREE-LEVEL CONSTRAINTS

From now on, we focus on the anomalous charm couplings $\kappa^{L,R}_{cd,cs,cb}$, neglecting the corresponding u and t anomalous couplings. To obtain constraints on the couplings, we begin by exploring their tree-level contributions to three different sets of processes, $D_{(s)} \to \ell\nu$, exclusive and inclusive $b \to c\ell^-\bar{\nu}$ transitions, and mixing-induced CP violation in $B \to J/\psi K$ and $B \to \eta_c K$, where the couplings may play some interesting roles.

A. D, $D_s \to \ell\nu$

From the Lagrangian in Eq. (1), at tree level one derives the decay rate

$$\Gamma(D \to \ell\nu) = \frac{G_F^2 f_D^2 m_\ell^2 m_D}{8\pi}\left(1 - \frac{m_\ell^2}{m_D^2}\right)^2 |V_{cd}(1 + \kappa^L_{cd} - \kappa^R_{cd})|^2, \tag{11}$$

where the decay constant f_D is defined by $\langle 0|\bar{d}\gamma^\mu c|D(p)\rangle = if_D p^\mu$. Changing V_{cd}, $\kappa^{L,R}_{cd}$, m_D, and f_D to V_{cs}, $\kappa^{L,R}_{cs}$, m_{D_s} and f_{D_s}, respectively, one obtains the decay width $\Gamma(D_s \to \ell\nu)$.

Recent measurements of D, $D_s \to \ell\nu$ yield [13,14]

$$f_D^{\rm exp} = (205.8 \pm 8.9)\ \text{MeV}, \qquad f_{D_s}^{\rm exp} = (261.2 \pm 6.9)\ \text{MeV}, \tag{12}$$

whereas SM calculations give [15,16]

$$f_D^{\rm th} = (202 \pm 8)\ \text{MeV}, \qquad f_{D_s}^{\rm th} = (240 \pm 7)\ \text{MeV}. \tag{13}$$

Evidently, for $D \to \ell\nu$ the data agree with theoretical predictions well, but for $D_s \to \ell\nu$ there is deviation at the 2-sigma level. It has been argued that this deviation may be due to physics beyond the SM [15], but it is too early to conclude that new physics is needed.

Nevertheless, one can turn the argument around to constrain new physics by assuming that the discrepancy between the calculated and measured values of the decay constants arose from the anomalous couplings, as the $\Gamma(D_{(s)} \to \ell\nu)$ formulas would imply. Using the experimental and theoretical numbers above, one can then extract

$$|\text{Re}(\kappa^L_{cd} - \kappa^R_{cd})| \leq 0.04, \tag{14}$$

$$0 \leq \text{Re}(\kappa^L_{cs} - \kappa^R_{cs}) \leq 0.1. \tag{15}$$

B. Semileptonic B decay and extraction of V_{cb}

The interaction in Eq. (1) will also affect the extraction of V_{cb} from semileptonic B decay. At the quark level, the effect of the new couplings is to scale the hadronic vector and axial-vector currents by the factors $1 + \kappa^{\rm L}_{cb} \pm \kappa^{\rm R}_{bc}$, respectively. This has the following implications.

First, the semileptonic exclusive decay $\bar{B} \to De\bar{\nu}_e$ is sensitive only to the vector form factor, and thus the differential (and total) decay rate simply gets multiplied by $|1 + \kappa^{\rm L}_{cb} + \kappa^{\rm R}_{bc}|^2$. To linear order in the κ's, this means that what is measured in this mode is

$$V^{\rm eff}_{cb} = V_{cb}(1 + {\rm Re}\kappa^{\rm L}_{cb} + {\rm Re}\kappa^{\rm R}_{cb}) = (39.4 \pm 4.4) \times 10^{-3}. \tag{16}$$

The number above and the other ones below for $V^{\rm eff}_{cb}$ are quoted from Ref. [17], and their errors result from adding the experimental and theoretical uncertainties given therein in quadrature.

Second, the semileptonic exclusive decay $\bar{B} \to D^* e\bar{\nu}_e$ is sensitive to both the vector and axial-vector currents. In the heavy-quark limit, $w = v \cdot v' = 1$ (where v and v' are the four-velocities of the B and D^*, respectively), only the axial-vector current survives [18], and so the decay rate in this limit would simply get multiplied by $|1 + \kappa^{\rm L}_{cb} - \kappa^{\rm R}_{bc}|^2$. One can do better than this by considering the form factors in the heavy-quark effective theory (HQET) where they either vanish or can be written in terms of the Isgur-Wise function $\xi(w)$ with the normalization $\xi(1) = 1$ [18]. Treating the form factors as constants throughout the kinematically allowed range $1 \le w \le 1.5$, one then finds to linear order in κ

$$\begin{aligned} V^{\rm eff}_{cb} &= V_{cb}(1 + {\rm Re}\kappa^{\rm L}_{cb} - 0.93\,{\rm Re}\kappa^{\rm R}_{cb}) \\ &= (38.6 \pm 1.4) \times 10^{-3}. \end{aligned} \tag{17}$$

Third, the semileptonic inclusive decay rate can be easily calculated to be

$$\begin{aligned} \Gamma(b \to ce^-\bar{\nu}_e) = \frac{G_{\rm F}^2 m_b^5}{192\pi^3}|V_{cb}|^2\{F(r)(|1 + \kappa^{\rm L}_{cb}|^2 + |\kappa^{\rm R}_{cb}|^2) \\ + 2G(r)\,{\rm Re}[(1 + \kappa^{\rm L}_{cb})\kappa^{\rm R*}_{cb}]\}, \end{aligned} \tag{18}$$

where $r = m_c/m_b \simeq 0.3$,

$$\begin{aligned} F(r) &= 1 - 8r^2 + 8r^6 - r^8 - 24r^4 \ln r, \\ G(r) &= -8r[1 + 9r^2 - 9r^4 - r^6 + 12r^2(1 + r^2)\ln r]. \end{aligned} \tag{19}$$

It follows that to linear order in κ

$$\begin{aligned} V^{\rm eff}_{cb} &= V_{cb}(1 + {\rm Re}\kappa^{\rm L}_{cb} - 1.5\,{\rm Re}\kappa^{\rm R}_{cb}) \\ &= (41.6 \pm 0.6) \times 10^{-3}. \end{aligned} \tag{20}$$

From these results it is evident that it is not possible to extract a bound on $\kappa^{\rm L}_{cb}$ (as long as quadratic effects are ignored), but we can extract bounds on $\kappa^{\rm R}_{cb}$. For example, we can do a two-parameter fit to Eqs. (16), (17), and (20) to find a χ^2 minimum for

$$V_{cb}(1 + {\rm Re}\kappa^{\rm L}_{cb}) = 0.038, \qquad {\rm Re}\kappa^{\rm R}_{cb} = -0.057, \tag{21}$$

with a corresponding 68% C.L. interval (1-σ error)

$$-0.13 \le {\rm Re}\kappa^{\rm R}_{cb} \le 0. \tag{22}$$

C. CP violation in $B \to J/\psi K$ and $B \to \eta_c K$

One of the decay modes expected to provide a clean determination of the unitarity-triangle parameter β from the measurement of time-dependent CP violation is $B \to \eta_c K$, just like $B \to J/\psi K$. The SM predicts the same $\sin(2\beta)$ for the two processes, whereas the current data for its effective values are [19]

$$\begin{aligned} \sin(2\beta^{\rm eff}_{\psi K}) &= 0.657 \pm 0.025, \\ \sin(2\beta^{\rm eff}_{\eta_c K}) &= 0.93 \pm 0.17, \end{aligned} \tag{23}$$

which disagree with each other at the 1.5 sigma level. Once again we can use the difference between the two measurements to constrain the new physics parametrized by the anomalous couplings. Since $\sin(2\beta^{\rm eff})$ measures the difference between the phase of the B-mixing matrix element and the phase of the ratio of amplitudes for the B decay and its antiparticle decay [20], then the discrepancy in $\beta^{\rm eff}$ between the two modes must arise from a difference between the phases of their amplitude ratios.

The effective Hamiltonian for the $b \to sc\bar{c}$ transition including the contribution of anomalous couplings can be written as

$$\begin{aligned} \mathcal{H}_{b\to sc\bar{c}} = \frac{4G_{\rm F}}{\sqrt{2}} V^*_{cs}V_{cb}(C_1\bar{c}\gamma^\mu P_{\rm L}c\bar{s}\gamma_\mu P_{\rm L}b \\ + C_2\bar{s}\gamma^\mu P_{\rm L}c\bar{c}\gamma_\mu P_{\rm L}b \\ + C_1^{\rm LR}\bar{s}_m\gamma^\mu P_{\rm L}c_n\bar{c}_n\gamma_\mu P_{\rm R}b_m \\ + C_2^{\rm LR}\bar{s}\gamma^\mu P_{\rm L}c\bar{c}\gamma_\mu P_{\rm R}b \\ + C_1^{\rm RL}\bar{s}_m\gamma^\mu P_{\rm R}c_n\bar{c}_n\gamma_\mu P_{\rm L}b_m \\ + C_2^{\rm RL}\bar{s}\gamma^\mu P_{\rm R}c\bar{c}\gamma_\mu P_{\rm L}b), \end{aligned} \tag{24}$$

where $C_{1,2}^{\rm (LR,RL)}$ are the Wilson coefficients, m and n are color indices, and we have neglected penguin operators. To linear order in κ, the Wilson coefficients at the m_W scale are $C_2(m_W) = 1 + \kappa^{\rm L*}_{cs} + \kappa^{\rm L}_{cb}$, $C_2^{\rm LR}(m_W) = \kappa^{\rm R}_{cb}$, and $C_2^{\rm RL}(m_W) = \kappa^{\rm R*}_{cs}$. These can be evolved down to a renormalization scale $\mu \sim m_b$ to become [21,22]

$$C_1(\mu) = \tfrac{1}{2}(\eta^{6/23} - \eta^{-12/23})C_2(m_W),$$
$$C_2(\mu) = \tfrac{1}{2}(\eta^{6/23} + \eta^{-12/23})C_2(m_W),$$
$$C_1^{\mathrm{LR,RL}}(\mu) = \tfrac{1}{3}(\eta^{-24/23} - \eta^{3/23})C_2^{\mathrm{LR,RL}}(m_W),$$
$$C_2^{\mathrm{LR,RL}}(\mu) = \eta^{3/23}C_2^{\mathrm{LR,RL}}(m_W) \tag{25}$$

at leading order in QCD, where $\eta = \alpha_s(m_W)/\alpha_s(\mu)$,

To determine the amplitudes for $\bar{B} \to J/\psi\bar{K}$, $\eta_c\bar{K}$, we adopt the naive factorization approximation. The relevant matrix elements and parameter values are collected in Appendix C. It follows that

$$\mathcal{M}(\bar{B}^0 \to \psi\bar{K}^0) = \sqrt{2}G_F V_{cs}^* V_{cb}(1 + \kappa_{cs}^{L*} + \kappa_{cb}^{L}) \times a_1 f_\psi m_\psi F_1^{BK} \varepsilon_\psi \cdot p_K,$$
$$\mathcal{M}(\bar{B}^0 \to \eta_c\bar{K}^0) = \frac{iG_F}{\sqrt{2}} V_{cs}^* V_{cb}\Big[(1 + \kappa_{cs}^{L*} + \kappa_{cb}^{L})a_1 + \frac{(a_1^{\mathrm{LR}} - a_1^{\mathrm{RL}})m_{\eta_c}^2}{m_c(m_b - m_s)}\Big](m_B^2 - m_K^2) f_{\eta_c} F_0^{BK}, \tag{26}$$

where

$$a_1 = C_1 + \frac{C_2}{N_c}, \qquad a_1^{\mathrm{LR,RL}} = C_1^{\mathrm{LR,RL}} + \frac{C_2^{\mathrm{LR,RL}}}{N_c}. \tag{27}$$

The presence of the second term in the $\bar{B} \to \eta_c\bar{K}$ amplitude offers the possibility of $\sin(2\beta^{\mathrm{eff}})$ in this decay mode being different from that in $\bar{B} \to J/\psi\bar{K}$. Defining

$$r_\kappa(\mu) = \frac{(a_1^{\mathrm{LR}}(\mu) - a_1^{\mathrm{RL}}(\mu))m_{\eta_c}^2}{a_1(\mu)m_c(\mu)(m_b(\mu) - m_s(\mu))}, \tag{28}$$

we then obtain to first order in κ

$$\beta_{\eta_c K}^{\mathrm{eff}} = \beta_{\psi K}^{\mathrm{eff}} + \arg(1 + r_\kappa) \simeq \beta_{\psi K}^{\mathrm{eff}} + \mathrm{Im} r_\kappa. \tag{29}$$

Taking $\mu = m_b = 4.2$ GeV and $N_c = 3$, we find $a_1(\mu) = 0.076$ and $r_\kappa(\mu) \simeq 20(\kappa_{cb}^{R} - \kappa_{cs}^{R*})$. Since the experimental numbers in Eq. (23) imply

$$\beta_{\eta_c K}^{\mathrm{eff}} = 0.60 \pm 0.23, \qquad \beta_{\psi K}^{\mathrm{eff}} = 0.358 \pm 0.017, \tag{30}$$

in view of Eq. (29) we can then impose $-0.005 \le \mathrm{Im} r_\kappa(\mu) \le 0.4$, which leads to the bound $-2.5 \times 10^{-4} \le \mathrm{Im}(\kappa_{cb}^{R} + \kappa_{cs}^{R}) \le 0.02$.

It is well known, however, that this naive factorization procedure fails to reproduce the experimental branching ratios, which can be better fit with $N_c \simeq 2$ [23]. Using this value we obtain instead $r_\kappa(\mu) \simeq 8(\kappa_{cb}^{R} - \kappa_{cs}^{R*})$. This would increase the upper bound for $\mathrm{Im}(\kappa_{cb}^{R} + \kappa_{cs}^{R})$ above by about a factor of 2, within the intrinsic uncertainty of our calculation,

$$-5 \times 10^{-4} \le \mathrm{Im}(\kappa_{cb}^{R} + \kappa_{cs}^{R}) \le 0.04. \tag{31}$$

IV. CONSTRAINTS FROM DIPOLE PENGUIN OPERATORS

We turn next to constraints from the magnetic-penguin transitions $d \to d'\gamma$ and $d \to d'g$. The specific processes we discuss are $b \to s\gamma$, $d \to s\gamma$, the CP-violation parameters ϵ and ϵ' in kaon mixing and decay, and hyperon CP violation.

A. $b \to s\gamma$

Including the SM contribution, the effective Hamiltonian for $b \to s\gamma$ is

$$\mathcal{H}_{b\to s\gamma} = \frac{-eG_F}{4\sqrt{2}\pi^2} \sum_{q=u,c,t} \bar{s}\,\sigma^{\mu\nu}(F_L^q P_L + F_R^q P_R) b F_{\mu\nu}, \tag{32}$$

where to $\mathcal{O}(\kappa)$

$$F_L^q = V_{qs}^* V_{qb}[(1 + \kappa_{qs}^{L*} + \kappa_{qb}^{L})m_s F_0^{\mathrm{SM}}(x_q) + \kappa_{qs}^{R*} m_q F_0(x_q)],$$
$$F_R^q = V_{qs}^* V_{qb}[(1 + \kappa_{qs}^{L*} + \kappa_{qb}^{L})m_b F_0^{\mathrm{SM}}(x_q) + \kappa_{qb}^{R} m_q F_0(x_q)], \tag{33}$$

following from Eqs. (B1) and (B3). The corresponding expressions for $b \to sg$ are similar in form and follow from Eqs. (B2) and (B4).

The experimental data on $b \to s\gamma$ have been found to impose very strong constraints on $\kappa_{tb,ts}$, limiting them to below the few-percent level [3]. Since $V_{cs}^* V_{cb} \simeq -V_{ts}^* V_{tb}$ and $m_t \gg m_c$, the preceding equations indicate that, if all the κ's were comparable in size, the top contributions would be larger than the charm ones by almost 2 orders of magnitude. All this means that $b \to s\gamma$ offers relatively weak constraints on $\kappa_{cb,cs}$, with upper bounds at the level of $\mathcal{O}(1)$.

B. $s \to d\gamma$

In an analogous manner, the anomalous couplings contribute to the short-distance transition $s \to d\gamma$, but in this case the charm contribution is expected to be more important than the top one. At lower energies, C_γ and C_g mix because of QCD corrections. At $\mu = 1$ GeV we have [22]

$$C_\gamma(\mu) = \bar{\eta}^8 C_\gamma(m_W) + \tfrac{8}{3}(\bar{\eta}^7 - \bar{\eta}^8)C_g(m_W), \tag{34}$$

where

$$\bar{\eta} = \left(\frac{\alpha_s(m_W)}{\alpha_s(m_b)}\right)^{2/23}\left(\frac{\alpha_s(m_b)}{\alpha_s(m_c)}\right)^{2/25}\left(\frac{\alpha_s(m_c)}{\alpha_s(\mu)}\right)^{2/27}. \tag{35}$$

Numerically, keeping only the charm contributions yields

$$C_\gamma^{\pm}(\mu) = (-38 + 0.023i)(\kappa_{cs}^{R} \pm \kappa_{cd}^{R*}) \times 10^{-7}\ \mathrm{GeV}^{-1}. \tag{36}$$

Hyperon and kaon radiative-weak decays provide the relevant constraints, the former being somewhat stronger and yielding [24]

$$\frac{|C_\gamma^+(\mu)|}{8\pi^2 G_F} \leq 12 \text{ MeV}. \tag{37}$$

This translates into

$$|\kappa_{cd}^{R*} + \kappa_{cs}^{R}| \leq 3, \tag{38}$$

which is a very weak bound compared to Eqs. (14) and (15).

C. ϵ and ϵ'

The gluonic dipole operators contribute to the CP-violation parameters ϵ and ϵ' in kaon mixing and decay, respectively. Since Q_g^+ is parity conserving, it contributes to ϵ via long-distance effects [25,26]. Being parity violating, Q_g^- contributes to ϵ'. One finds [6,26,27]

$$\begin{aligned}(\epsilon)_\kappa &= -2.3 \times 10^5 \text{ GeV} B_\epsilon \, \text{Im} C_g^+(\mu), \\ \left(\frac{\epsilon'}{\epsilon}\right)_\kappa &= 4.4 \times 10^5 \text{ GeV} B_{\epsilon'} \, \text{Im} C_g^-(\mu),\end{aligned} \tag{39}$$

where the contributions of the anomalous charm couplings to $C_g^\pm$ are

$$\begin{aligned}C_g^\pm(\mu) &= \bar{\eta}^7 C_g^\pm(m_W) \\ &= (-21 + 0.013i)(\kappa_{cs}^R \pm \kappa_{cd}^{R*}) \times 10^{-7} \text{ GeV}^{-1}\end{aligned} \tag{40}$$

for $\mu = 1$ GeV and the hadronic uncertainties are represented by

$$0.2 \leq |B_\epsilon| \leq 1, \qquad 0.5 \leq |B_{\epsilon'}| \leq 2. \tag{41}$$

The experimental data are $|\epsilon| = (2.229 \pm 0.012) \times 10^{-3}$ and $\text{Re}(\epsilon'/\epsilon) = (1.65 \pm 0.26) \times 10^{-3}$ [13]. The SM predicts $|\epsilon|_{SM} = (2.06^{+0.47}_{-0.53}) \times 10^{-3}$ [28], but for ϵ' the SM calculation still involves a large uncertainty [29]. Consequently, we require that

$$|\epsilon|_\kappa < 0.7 \times 10^{-3}, \qquad \left(\frac{\epsilon'}{\epsilon}\right)_\kappa < 1.7 \times 10^{-3}. \tag{42}$$

The resulting constraints on $\kappa_{cd,cs}^R$ are complicated and will be presented in Fig. 2 in Sec. VII.

There are other loop-generated operators contributing to ϵ, and hence they provide more constraints on the anomalous charm couplings. These operators will be discussed in Sec. VI C.

D. Hyperon nonleptonic decays

Hyperon decays provide an additional environment to study CP-violating $|\Delta S| = 1$ interactions. The main observable of interest in this case is the CP-violating asymmetry $A = (\alpha + \bar{\alpha})/(\alpha - \bar{\alpha})$, where α is a decay parameter in the decay of a hyperon into another baryon and a spinless meson and $\bar{\alpha}$ is the corresponding parameter in the antiparticle process [30].

Experimentally, a preliminary value $A_{\Lambda\Xi}^{\text{exp}} = (-6 \pm 3) \times 10^{-4}$ for A measured in the decay chain $\bar{\Xi} \to \Lambda\pi \to p\pi\pi$ has recently been reported [31]. The SM prediction is $|A_{\bar{\Xi}\Lambda}^{SM}| \lesssim 5 \times 10^{-5}$ [30], which is an order of magnitude smaller than the central value of the measurement. Since this is only a 2-sigma disagreement, it is premature to attribute it to new physics. However, this difference can also be used to constrain the anomalous charm couplings.

The contribution of the gluonic dipole operators to the asymmetry $A_{\Lambda\Xi}$ has been estimated in Ref. [27]. The result can be written as

$$(A_{\Xi\Lambda})_\kappa = 10^5 B_+ \, \text{Im} C_g^+(\mu) + 10^5 B_- \, \text{Im} C_g^-(\mu), \tag{43}$$

where $C_g^\pm(\mu)$ due to the anomalous charm couplings are given in Eq. (40) and

$$-1.4 \leq B_+ \leq 0.5, \qquad -0.9 \leq B_- \leq 1.3 \tag{44}$$

reflect the hadronic uncertainties. The preliminary HyperCP result above suggests that

$$-9 \times 10^{-4} < (A_{\Xi\Lambda})_\kappa < -3 \times 10^{-4}. \tag{45}$$

The resulting constraints are shown in Fig. 2 in Sec. VII.

V. ELECTRIC DIPOLE MOMENT OF NEUTRON

The flavor-conserving counterparts of the magnetic-dipole operators discussed above contribute to the neutron EDM. The latter is described by the effective Lagrangian

$$\mathcal{L}_{n\text{edm}} = -\frac{i}{2} d_n \bar{n} \sigma^{\mu\nu} \gamma_5 n F_{\mu\nu}. \tag{46}$$

The dipole moments d_d^{edm} and d_d^{cdm} of the d quark in Eq. (7) contribute to d_n. Using the valence quark model, we have [8]

$$d_n^{(d)} = \tfrac{4}{3} d_d^{\text{edm}}(\mu) + \tfrac{4}{9} e d_d^{\text{cdm}}(\mu), \tag{47}$$

where at $\mu = 1$ GeV

$$\begin{aligned}d_d^{\text{edm}}(\mu) &= \bar{\eta}^8 d_d^{\text{edm}}(m_W) + \tfrac{8}{3}(\bar{\eta}^7 - \bar{\eta}^8) e d_d^{\text{cdm}}(m_W), \\ d_d^{\text{cdm}}(\mu) &= \bar{\eta}^7 d_d^{\text{cdm}}(m_W),\end{aligned} \tag{48}$$

with $\bar{\eta}$ being given in Eq. (35). The anomalous charm contribution is then

$$d_n^{(d)} = 6.9 \, \text{Im} \kappa_{cd}^R \times 10^{-22} e \text{ cm}. \tag{49}$$

Similarly, the electric and color dipole-moments of the s quark produced by the anomalous charm couplings are

$$d_s^{\rm edm}(\mu) = \frac{-eG_{\rm F}}{2\sqrt{2}\pi^2}|V_{cs}|^2\,{\rm Im}\kappa_{cs}^{\rm R} m_c\Big[\bar\eta^8 F_0(x_c) + \frac{8}{3}(\bar\eta^7 - \bar\eta^8)G_0(x_c)\Big],$$

$$d_s^{\rm cdm}(\mu) = -\bar\eta^7\frac{g_{\rm s}G_{\rm F}}{2\sqrt{2}\pi^2}|V_{cs}|^2\,{\rm Im}\kappa_{cs}^{\rm R} m_c G_0(x_c), \qquad (50)$$

and so their contribution to d_n is given by

$$d_n^{(s)} = B_{\rm e} d_s^{\rm edm}(\mu) + B_{\rm c} e d_s^{\rm cdm}(\mu) = (82B_{\rm e} + 46B_{\rm c})\,{\rm Im}\kappa_{cs}^{\rm R}\times 10^{-22} e\ {\rm cm}, \qquad (51)$$

where $-0.35 \le B_{\rm e} \le -0.01$ and $0.01 \le B_{\rm c} \le 0.26$ reflect the wide range of estimates for $d_n^{(s)}$ in the literature [10], in contrast to those for $d_n^{(d)}$. The combined contribution of $d_n^{(d,s)}$ is then

$$(d_n)_\kappa = d_n^{(d)} + d_n^{(s)} = (0.69\,{\rm Im}\kappa_{cd}^{\rm R} + B_n\,{\rm Im}\kappa_{cs}^{\rm R})\times 10^{-21} e\ {\rm cm}, \qquad (52)$$

where

$$-2.8 \le B_n \le +1.1. \qquad (53)$$

From the experimental bound $|d_n|_{\rm exp} < 2.9\times 10^{-26} e$ cm at 90% C.L. [13], we will impose the bound

$$|d_n|_\kappa < 2.9\times 10^{-26} e\ {\rm cm} \qquad (54)$$

in Sec. VII to restrict the anomalous couplings further.

The s-quark dipole moments $d_s^{\rm edm}$ and $d_s^{\rm edm}$ above also contribute to the EDM of the Λ hyperon and therefore may be constrained directly by experiment. However, the experimental limit, $d_\Lambda = (-3.0 \pm 7.4)\times 10^{-17} e$ cm [32] or $d_\Lambda < 1.5\times 10^{-16} e$ cm at 90% C.L. [13], is very weak compared to Eq. (54) and hence will not be used for constraining the couplings.

VI. OTHER LOOP CONSTRAINTS

In this section we explore several other processes where the anomalous charm couplings can contribute via penguin and box diagrams.

A. $K^+ \to \pi^+ \nu\bar\nu$

To quantify the contribution of the anomalous charm couplings to this mode, it is convenient to compare it with the dominant contribution in the SM. The latter comes from the top loop and is given by [21,33]

$$\mathcal{M}_{\rm SM}(K^+\to\pi^+\nu\bar\nu) = \frac{G_{\rm F}}{\sqrt{2}}\frac{\alpha}{2\pi\sin^2\theta_{\rm W}} V_{td}V_{ts}^* X_0(x_t) \times\langle\pi^+|\bar s\gamma_\mu d|K^+\rangle\bar\nu\gamma^\mu(1-\gamma_5)\nu, \qquad (55)$$

following from Eq. (B9), without QCD corrections. It is also convenient to neglect the masses of the leptons associated with the neutrinos in the new contribution, as in Eq. (8), so that we can work with just one of them. The total amplitude can thus be written in terms of the SM amplitude above as

$$\mathcal{M}(K^+\to\pi^+\nu\bar\nu) = (1+\delta)\mathcal{M}_{\rm SM}(K^+\to\pi^+\nu\bar\nu), \qquad (56)$$

where to linear order in κ

$$\delta = \frac{V_{cd}V_{cs}^*}{V_{td}V_{ts}^*}\frac{(\kappa_{cd}^{\rm L} + \kappa_{cs}^{\rm L*})[-3\ln(\Lambda/m_W) + 4X_0(x_c)]}{4X(x_t)}. \qquad (57)$$

In the above expression we have used $X(x_t) \simeq 1.4$ instead of $X_0(x_t)$ in the denominator to incorporate the QCD corrections in the SM [34]. The SM prediction for the branching ratio is $\mathcal{B}_{\rm SM}(K^+\to\pi^+\nu\bar\nu) = (8.5\pm 0.7)\times 10^{-11}$ [34], to be compared with its experimental value $\mathcal{B}_{\rm exp} = (1.73^{+1.15}_{-1.05})\times 10^{-10}$ [35]. Accordingly, we require $-0.2 \le {\rm Re}\delta \le 1$, which translates into

$$-2.5\times 10^{-4} \le -{\rm Re}(\kappa_{cd}^{\rm L} + \kappa_{cs}^{\rm L}) + 0.42\,{\rm Im}(\kappa_{cd}^{\rm L} - \kappa_{cs}^{\rm L}) \le 1.3\times 10^{-3}. \qquad (58)$$

It is interesting to compare the anomalous charm contribution to the SM charm contribution. Their ratio is

$$\frac{\mathcal{M}_\kappa(K^+\to\pi^+\nu\bar\nu)}{\mathcal{M}_{\rm SM}^{(c)}(K^+\to\pi^+\nu\bar\nu)} = \frac{(\kappa_{cd}^{\rm L} + \kappa_{cs}^{\rm L*})[-3\ln(\Lambda/m_W) + 4X_0(x_c)]}{4X_{\rm NL}}, \qquad (59)$$

where $6\times 10^{-4} \lesssim X_{\rm NL} \lesssim 1\times 10^{-3}$ incorporates QCD corrections and lepton-mass dependence [21]. With the $\kappa_{cd}^{\rm L} + \kappa_{cs}^{\rm L}$ at the upper end of the range above, the two contributions are similar in size. This implies that the current experimental situation admits a 100% uncertainty in the charm contribution to the branching ratio, much larger than the theoretical uncertainty within the SM.

Constraints on the anomalous couplings can also be extracted from the related B-meson modes, $B\to X\nu\bar\nu$, but the resulting bounds are about 3 orders of magnitude weaker due to unfavorable CKM angles. Experimentally, only upper limits for their decay rates are currently available [19]. For these reasons, we do not discuss them further.

B. $K_L \to \mu^+\mu^-$

The dominant part of the short-distance contribution to the SM amplitude for $K^0\to\mu^+\mu^-$ is again induced by the

top loop and can be expressed as [21,33]

$$\mathcal{M}^{\rm SD}_{\rm SM}(K^0 \to \mu^+\mu^-) = -\frac{G_{\rm F}}{\sqrt{2}}\frac{\alpha}{2\pi \sin^2\theta_{\rm W}} V_{td}V_{ts}^* Y_0(x_t) \times \langle 0|\bar{s}\gamma^\sigma\gamma_5 d|K^0\rangle \bar{\mu}\gamma_\sigma\gamma_5\mu, \quad (60)$$

from Eq. (9). Combining this with the anomalous charm contribution in Eq. (9), we arrive at the total short-distance amplitude

$$\mathcal{M}_{\rm SD}(K_L \to \mu^+\mu^-) = (1+\delta')\mathcal{M}^{\rm SD}_{\rm SM}(K_L \to \mu^+\mu^-), \quad (61)$$

where to linear order in κ

$$\delta' = \frac{{\rm Re}[V_{cd}^* V_{cs}(\kappa^{\rm L}_{cs} + \kappa^{\rm L*}_{cd})][-3\ln(\Lambda/m_W) + 4Y_0(x_c)]}{4\,{\rm Re}(V_{td}^* V_{ts})Y(x_t)}, \quad (62)$$

with $Y(x_t) \simeq 0.95$ being the QCD-corrected value of $Y_0(x_t)$ [36]. Since the measured branching ratio, $\mathcal{B}(K_L \to \mu^+\mu^-) = (6.84 \pm 0.11)\times 10^{-9}$ [13], is almost saturated by the absorptive part of the long-distance contribution, $\mathcal{B}_{\rm abs} = (6.64 \pm 0.07)\times 10^{-9}$ [37], the difference between them suggests the allowed room for new physics, $\mathcal{B}_{\rm NP} \lesssim 3.8\times 10^{-10}$, the upper bound being about one half of the SM short-distance contribution, $\mathcal{B}^{\rm SD}_{\rm SM} = (7.9 \pm 1.2)\times 10^{-10}$ [36]. Consequently, we demand $|\delta'| \le 0.2$, which implies

$$|{\rm Re}(\kappa^{\rm L}_{cs} + \kappa^{\rm L}_{cd}) + 6\times 10^{-4}\,{\rm Im}(\kappa^{\rm L}_{cs} - \kappa^{\rm L}_{cd})| \le 1.5\times 10^{-4}. \quad (63)$$

One could also carry out a similar analysis as above for $B \to \ell^+\ell^-$, but the CKM angles in that case are such that the constraints would be much weaker. In addition, only experimental bounds on the rates are currently available [19].

C. K-$\bar{K}$ mixing

The matrix element M_{12} for K^0-$\bar{K}^0$ mixing is defined by [21]

$$2m_K M^K_{12} = \langle K^0|\mathcal{H}_{d\bar{s}\to\bar{d}s}|\bar{K}^0\rangle \quad (64)$$

where the effective Hamiltonian $\mathcal{H}_{d\bar{s}\to\bar{d}s}$ consists of SM and new-physics terms. For the latter, the contribution of the anomalous charm couplings can be derived from Eq. (10), where the last line is negligible compared to the second because of the smallness of x_c. Thus

$$\begin{aligned} M^{K,\kappa}_{12} &= \frac{G_{\rm F}^2 m_W^2}{24\pi^2} f_K^2 m_K \lambda_c^{ds}\Big[\bar{\eta}^3 B_K(\kappa^{\rm L*}_{cd} + \kappa^{\rm L}_{cs}) \\ &\quad\times\left(-\lambda_t^{ds} x_t \ln\frac{\mu^2}{m_W^2} - \sum_q \lambda_q^{ds}\mathcal{B}_1(x_q, x_c)\right) \\ &\quad + \frac{\bar{\eta}^{3/2} B_K m_K^2}{(m_d+m_s)^2}\kappa^{\rm R*}_{cd}\kappa^{\rm R}_{cs} \\ &\quad\times\left(\lambda_t^{ds} x_t \ln\frac{\mu^2}{m_W^2} + \sum_q \lambda_q^{ds}\mathcal{B}_2(x_q, x_c)\right)\Big] \\ &= -(0.090 + 0.031i)\ {\rm ps}^{-1}(\kappa^{\rm L*}_{cd} + \kappa^{\rm L}_{cs}) \\ &\quad + (2.1 + 0.58i)\ {\rm ps}^{-1}\kappa^{\rm R*}_{cd}\kappa^{\rm R}_{cs}, \end{aligned} \quad (65)$$

where $\lambda_q^{ds} = V_{qd}^* V_{qs}$, we have included QCD-correction factors at leading order with $\bar{\eta}$ given in Eq. (35), $m_d(\mu) + m_s(\mu) = 142$ MeV at $\mu = 1$ GeV, and the other parameters can be found in Appendix C. Evidently, the inclusion of the second term in $M^{K,\kappa}_{12}$, albeit quadratic in $\kappa^{\rm R}$, is important as it receives large chiral and QCD enhancement with respect to the first term.

Now, the difference ΔM_K between the K_L and K_S masses is related to $M^K_{12} = M^{K,{\rm SM}}_{12} + M^{K,\kappa}_{12}$ by $\Delta M_K = 2\,{\rm Re}M^K_{12} + \Delta M^{\rm LD}_K$, the long-distance term $\Delta M^{\rm LD}_K$ being sizable [21]. Since the LD part suffers from significant uncertainties, we constrain the anomalous couplings by requiring that their contribution to ΔM_K be less than the largest SM contribution, which comes from the charm loop and is given by

$$M^{K,{\rm SM}}_{12} \simeq \frac{G_{\rm F}^2 m_W^2}{12\pi^2} f_K^2 m_K B_K \eta_{cc}(\lambda_c^{ds})^2 S_0(x_c), \quad (66)$$

with the parameter values in Appendix C. The result is

$$\begin{aligned} &|0.043\,{\rm Re}(\kappa^{\rm L}_{cd} + \kappa^{\rm L}_{cs}) + 0.015\,{\rm Im}(\kappa^{\rm L}_{cd} - \kappa^{\rm L}_{cs}) \\ &\quad - {\rm Re}(\kappa^{\rm R*}_{cd}\kappa^{\rm R}_{cs}) + 0.28\,{\rm Im}(\kappa^{\rm R*}_{cd}\kappa^{\rm R}_{cs})| \\ &\quad \le 8.5\times 10^{-4}. \end{aligned} \quad (67)$$

A complementary constraint on the couplings can be obtained from the CP-violation parameter ϵ. Its magnitude is related to M^K_{12} by [21]

$$|\epsilon| \simeq \frac{|{\rm Im}M^K_{12}|}{\sqrt{2}\Delta M_K^{\rm exp}}, \quad (68)$$

where $\Delta M_K^{\rm exp} = (3.483 \pm 0.006)\times 10^{-15}$ GeV [13] and the small term containing the CP-violating phase in the $K \to \pi\pi$ amplitude has been dropped. Since $|\epsilon|_{\rm exp} = (2.229 \pm 0.012)\times 10^{-3}$ [13] and $|\epsilon|_{\rm SM} = (2.06^{+0.47}_{-0.53})\times 10^{-3}$ [28], we again demand $|\epsilon|_\kappa < 0.7\times 10^{-3}$ for the contribution in Eq. (65). This translates into

$$|0.015\,\mathrm{Re}(\kappa^{\mathrm{L}}_{cs}+\kappa^{\mathrm{L}}_{cd})+0.043\,\mathrm{Im}(\kappa^{\mathrm{L}}_{cs}-\kappa^{\mathrm{L}}_{cd}) - 0.28\,\mathrm{Re}(\kappa^{\mathrm{R}*}_{cd}\kappa^{\mathrm{R}}_{cs})-\mathrm{Im}(\kappa^{\mathrm{R}*}_{cd}\kappa^{\mathrm{R}}_{cs})| \le 2.5\times10^{-6}. \quad (69)$$

D. B_d-$\bar{B}_d$ mixing

In the SM the matrix element M^d_{12} for B^0_d-$\bar{B}^0_d$ mixing is dominated by the top-loop contribution and given by [21]

$$M^{d,\mathrm{SM}}_{12}=\frac{\langle B^0_d|\mathcal{H}^{\mathrm{SM}}_{d\bar{b}\to\bar{d}b}|\bar{B}^0_d\rangle}{2m_{B_d}} \simeq \frac{G_{\mathrm{F}}^2m_W^2}{12\pi^2}f^2_{B_d}m_{B_d}\eta_B B_{B_d}(V_{tb}V^*_{td})^2S_0(x_t) \quad (70)$$

following from Eq. (B18), where a QCD-correction factor η_B has been included and the parameter values can be found in Appendix C. In contrast, since $V^*_{cd}V_{cb}$ and $V^*_{td}V_{tb}$ are comparable in size, the anomalous couplings of charm and top may produce similar effects on M^d_{12}, as can be inferred from Eq. (10). The anomalous top contributions to B mixing having been studied before [38], we switch them off and get, to linear order in κ,

$$M^{d,\kappa}_{12}=\frac{G_{\mathrm{F}}^2m_W^2}{24\pi^2}f^2_{B_d}m_{B_d}\eta_B B_{B_d}\lambda^{db}_c(\kappa^{\mathrm{L}}_{cb}+\kappa^{\mathrm{L}*}_{cd}) \times\left(-\lambda^{db}_t x_t\ln\frac{\Lambda^2}{m_W^2}-\sum_q\lambda^{db}_q\mathcal{B}_1(x_q,x_c)\right) = (1.6+0.63i)\ \mathrm{ps}^{-1}(\kappa^{\mathrm{L}}_{cb}+\kappa^{\mathrm{L}*}_{cd}), \quad (71)$$

where $\lambda^{db}_q=V^*_{qd}V_{qb}$ and we have neglected the terms quadratic in κ^{R} because their quark operators do not get as much chiral and QCD enhancement as those in the kaon-mixing case.

The difference ΔM_d between the masses of the heavy and light mass-eigenstates is related to $M^d_{12}=M^{d,\mathrm{SM}}_{12}+M^{d,\kappa}_{12}$ by $\Delta M_d=2|M^d_{12}|$ [21]. The measured value $\Delta M^{\mathrm{exp}}_d=(0.507\pm0.005)\ \mathrm{ps}^{-1}$ [13] agrees with the SM prediction, $\Delta M^{\mathrm{SM}}_d=(0.563^{+0.068}_{-0.076})\ \mathrm{ps}^{-1}$ [28]. In the presence of the anomalous couplings, these numbers are related by

$$\Delta M^{\mathrm{exp}}_d=\Delta M^{\mathrm{SM}}_d|1+\delta_d|, \qquad \delta_d=\frac{M^{d,\kappa}_{12}}{M^{d,\mathrm{SM}}_{12}}. \quad (72)$$

Accordingly, we impose $-0.2\le\mathrm{Re}\,\delta_d\le+0.02$, which leads to

$$-0.031\le\mathrm{Re}(\kappa^{\mathrm{L}}_{cb}+\kappa^{\mathrm{L}}_{cd})+0.4\,\mathrm{Im}(\kappa^{\mathrm{L}}_{cb}-\kappa^{\mathrm{L}}_{cd})\le0.003. \quad (73)$$

An additional constraint can be extracted from the β measurement in $B\to J/\psi K$. The anomalous couplings enter β^{eff} via both the mixing and decay amplitudes. Since the mixing parameters p_{B_d} and q_{B_d} are related to M^d_{12} by $q_{B_d}/p_{B_d}\simeq M^{d*}_{12}/|M^d_{12}|$ [20], we have

$$\frac{q_{B_d}}{p_{B_d}}\simeq\sqrt{\frac{M^{d,\mathrm{SM}*}_{12}(1+\delta^*_d)}{M^{d,\mathrm{SM}}_{12}(1+\delta_d)}}\simeq\frac{V_{td}V^*_{tb}}{V^*_{td}V_{tb}}e^{-i\,\mathrm{Im}\delta_d}. \quad (74)$$

From the decay amplitude in Eq. (26), we derive

$$\frac{\mathcal{M}(\bar{B}^0\to\psi K_S)}{\mathcal{M}(B^0\to\psi K_S)}=-\frac{V^*_{cd}V_{cb}(1+\kappa^{\mathrm{L}*}_{cs}+\kappa^{\mathrm{L}}_{cb})}{V_{cd}V^*_{cb}(1+\kappa^{\mathrm{L}}_{cs}+\kappa^{\mathrm{L}*}_{cb})} \simeq-\frac{V^*_{cd}V_{cb}}{V_{cd}V^*_{cb}}[1+2i\,\mathrm{Im}(\kappa^{\mathrm{L}}_{cb}-\kappa^{\mathrm{L}}_{cs})], \quad (75)$$

having incorporated the K-mixing factor $q_K/p_K=V^*_{cd}V_{cs}/(V_{cd}V^*_{cs})$ [20]. It follows that

$$e^{-2i\beta^{\mathrm{eff}}_{\psi K}}=\frac{q_{B_d}}{p_{B_d}}\frac{\mathcal{M}(\bar{B}^0\to\psi K_S)}{\mathcal{M}(B^0\to\psi K_S)} \simeq e^{-2i\beta^{\mathrm{SM}}}e^{2i\,\mathrm{Im}(\kappa^{\mathrm{L}}_{cb}-\kappa^{\mathrm{L}}_{cs})-i\,\mathrm{Im}\delta_d}. \quad (76)$$

Upon comparing the experimental value $2\beta^{\mathrm{eff}}=2\beta^{\mathrm{eff}}_{\psi K}=0.717\pm0.033$ from Eq. (30) to the SM prediction $2\beta^{\mathrm{SM}}=0.753^{+0.032}_{-0.028}$ [28], we then require $-0.01\le2\,\mathrm{Im}(\kappa^{\mathrm{L}}_{cb}-\kappa^{\mathrm{L}}_{cs})-\mathrm{Im}\delta_d\le0.08$, which implies

$$-1.5\times10^{-3}\le0.4\,\mathrm{Re}(\kappa^{\mathrm{L}}_{cb}+\kappa^{\mathrm{L}}_{cd})-0.69\,\mathrm{Im}\kappa^{\mathrm{L}}_{cb} +\mathrm{Im}\kappa^{\mathrm{L}}_{cd}-0.31\,\mathrm{Im}\kappa^{\mathrm{L}}_{cs} \le0.012. \quad (77)$$

E. B_s-$\bar{B}_s$ mixing

The SM part of the matrix element M^s_{12} for B^0_s-$\bar{B}^0_s$ mixing is also dominated by the top contribution [21],

$$M^{s,\mathrm{SM}}_{12}\simeq\frac{G_{\mathrm{F}}^2m_W^2}{12\pi^2}f^2_{B_s}m_{B_s}\eta_B B_{B_s}(V_{tb}V^*_{ts})^2S_0(x_t). \quad (78)$$

For the anomalous couplings, again the charm contribution alone is

$$M^{s,\kappa}_{12}=\frac{G_{\mathrm{F}}^2m_W^2}{24\pi^2}f^2_{B_s}m_{B_s}\eta_B B_{B_s}\lambda^{sb}_c(\kappa^{\mathrm{L}}_{cb}+\kappa^{\mathrm{L}*}_{cs}) \times\left(-\lambda^{sb}_t x_t\ln\frac{\Lambda^2}{m_W^2}-\sum_q\lambda^{sb}_q\mathcal{B}_1(x_q,x_c)\right) = (53-0.95i)\ \mathrm{ps}^{-1}(\kappa^{\mathrm{L}}_{cb}+\kappa^{\mathrm{L}*}_{cs}), \quad (79)$$

where $\lambda^{sb}_q=V^*_{qs}V_{qb}$.

Similarly to the B_d case, we have here

$$\Delta M^{\mathrm{exp}}_s=\Delta M^{\mathrm{SM}}_s|1+\delta_s|, \qquad \delta_s=\frac{M^{s,\kappa}_{12}}{M^{s,\mathrm{SM}}_{12}}. \quad (80)$$

The experimental value, $\Delta M^{\mathrm{exp}}_s=(17.77\pm0.12)\ \mathrm{ps}^{-1}$ [13], is in agreement with the SM prediction, $\Delta M^{\mathrm{SM}}_s=(17.6^{+1.7}_{-1.8})\ \mathrm{ps}^{-1}$ [28]. These numbers allow us to require

$-0.09 \leq \mathrm{Re}\delta_s \leq 0.1$, leading to

$$-0.014 \leq \mathrm{Re}(\kappa^{\mathrm{L}}_{cs} + \kappa^{\mathrm{L}}_{cb}) + 0.018\,\mathrm{Im}(\kappa^{\mathrm{L}}_{cs} - \kappa^{\mathrm{L}}_{cb}) \leq 0.015. \quad (81)$$

A complementary constraint is provided by the parameter β_s in B_s decay, analogously to β in B_d decay. In this case, the mode of interest is $\bar{B}^0_s \to J/\psi\phi$, which proceeds from the same $b \to sc\bar{c}$ transition as $\bar{B}^0_d \to J/\psi\bar{K}$. For the mixing factor, we have

$$\frac{q_{B_s}}{p_{B_s}} \simeq \sqrt{\frac{M^{s,\mathrm{SM}*}_{12}(1+\delta^*_s)}{M^{s,\mathrm{SM}}_{12}(1+\delta_s)}} \simeq \frac{V_{ts}V^*_{tb}}{V^*_{ts}V_{tb}}\, e^{-i\,\mathrm{Im}\delta_s}, \quad (82)$$

and for the ratio of decay amplitudes, as in Eq. (75),

$$\frac{\mathcal{M}(\bar{B}^0_s \to (J/\psi\phi)_f)}{\mathcal{M}(B^0_s \to (J/\psi\phi)_f)} \simeq \eta_f \frac{V^*_{cs}V_{cb}}{V_{cs}V^*_{cb}}[1 + 2i\,\mathrm{Im}(\kappa^{\mathrm{L}}_{cb} - \kappa^{\mathrm{L}}_{cs})], \quad (83)$$

where $(J/\psi\phi)_f$ is one of the CP eigenstates of the $J/\psi\phi$ final-state and η_f its CP eigenvalue. It follows that

$$e^{2i\beta^{\mathrm{eff}}_{\psi\phi}} = -\eta_f \frac{q_{B_s}}{p_{B_s}} \frac{\mathcal{M}(\bar{B}^0_s \to (J/\psi\phi)_f)}{\mathcal{M}(B^0_s \to (J/\psi\phi)_f)} \simeq e^{2i\beta^{\mathrm{SM}}_s} e^{2i\,\mathrm{Im}(\kappa^{\mathrm{L}}_{cb} - \kappa^{\mathrm{L}}_{cs}) - i\,\mathrm{Im}\delta_s}. \quad (84)$$

The SM yields $2\beta^{\mathrm{SM}}_s = 0.03614^{+0.00172}_{-0.00162}$ [28], but the measurements of $B_s \to J/\psi\phi$ yield the average value $2\beta^{\mathrm{eff}}_s = 2\beta^{\mathrm{eff}}_{\psi\phi} = 0.77^{+0.37}_{-0.29}$ or $2.36^{+0.29}_{-0.37}$ [19]. It is again too early to attribute this difference to new physics, but it can be used to impose the bound $-0.003 \leq 2\,\mathrm{Im}(\kappa^{\mathrm{L}}_{cb} - \kappa^{\mathrm{L}}_{cs}) - \mathrm{Im}\delta_s \leq 0.4$, which yields

$$-0.09 \leq 0.026\,\mathrm{Re}(\kappa^{\mathrm{L}}_{cb} + \kappa^{\mathrm{L}}_{cs}) + \mathrm{Im}(\kappa^{\mathrm{L}}_{cb} - \kappa^{\mathrm{L}}_{cs}) \leq 7 \times 10^{-4}. \quad (85)$$

VII. SUMMARY AND CONCLUSIONS

We have explored the phenomenological consequences of anomalous W-boson couplings to the charm quark in a comprehensive way. Most of the constraints we have obtained are summarized in Table I. In writing them, we have followed the discussion in Appendix A about the independent parameters in the quark-mixing matrices and chosen $\arg\kappa^{\mathrm{L}}_{cd} = 0$. Consequently, we have used the condition $\mathrm{Im}\kappa^{\mathrm{L}}_{cd} = 0$ in all the results. All the constraints in this table are quoted as 1-σ errors, but in some cases the theoretical error is only an order of magnitude and this is not reflected in the quoted range. The discussion in the text makes it clear whenever this happens. We leave out from the table the processes $b \to s\gamma$ and $s \to d\gamma$ since the resulting bounds are not competitive with the rest.

In Fig. 1 we show the parameter space of the real and imaginary parts of κ^{L}_{cs} and κ^{L}_{cb} assuming that only one of them is nonzero at a time. This figure indicates that currently the phase of κ^{L}_{cs} is only loosely constrained and ranges from $-90°$ to $90°$. In contrast, the phase of κ^{L}_{cb} is unconstrained if its magnitude is small (at the 10^{-3} level). However, larger values of $|\kappa^{\mathrm{L}}_{cb}|$, at the few percent level, are also allowed provided its phase lies in a range roughly between $-150°$ and $-56°$.

We treat the constraints arising from the contributions of magnetic-dipole operators to CP-violating observables separately and display those in Fig. 2. These observables receive contributions from the anomalous couplings $\mathrm{Im}\kappa^{\mathrm{R}}_{cd,cs}$ that are much larger than SM contributions to the dipole operators. These enhanced contributions to ϵ, ϵ', the neutron EDM, and $A_{\Xi\Lambda}$ have been studied before as they arise within LR models and supersymmetry [6,26,39].

The calculations for all of these CP-violating observables suffer from large theoretical uncertainties which we have parametrized with B factors in this paper. For illustration, we display two plots in Fig. 2 resulting from choosing two representative sample sets of values of the parameters $B_{\epsilon,\epsilon',+,-,n}$ within their ranges in Eqs. (41), (44),

TABLE I. Summary of constraints, with their equation numbers, from various processes.

Process	Eq.	Constraint	#
$D \to \ell\nu$	(14)	$\lvert\mathrm{Re}(\kappa^{\mathrm{L}}_{cd} - \kappa^{\mathrm{R}}_{cd})\rvert \leq 0.04$	1
$D_s \to \ell\nu$	(15)	$0 \leq \mathrm{Re}(\kappa^{\mathrm{L}}_{cs} - \kappa^{\mathrm{R}}_{cs}) \leq 0.1$	2
$b \to c\ell\bar{\nu}$	(22)	$-0.13 \leq \mathrm{Re}\kappa^{\mathrm{R}}_{cb} \leq 0$	3
$B \to J/\psi K,\ \eta_c K$	(31)	$-5 \times 10^{-4} \leq \mathrm{Im}(\kappa^{\mathrm{R}}_{cb} + \kappa^{\mathrm{R}}_{cs}) \leq 0.04$	4
$K^+ \to \pi^+\nu\bar{\nu}$	(58)	$-1.3 \times 10^{-3} \leq \mathrm{Re}(\kappa^{\mathrm{L}}_{cd} + \kappa^{\mathrm{L}}_{cs}) + 0.42\,\mathrm{Im}\kappa^{\mathrm{L}}_{cs} \leq 2.5 \times 10^{-4}$	5
$K_L \to \mu^+\mu^-$	(63)	$\lvert\mathrm{Re}(\kappa^{\mathrm{L}}_{cs} + \kappa^{\mathrm{L}}_{cd}) + 6 \times 10^{-4}\,\mathrm{Im}\kappa^{\mathrm{L}}_{cs}\rvert \leq 1.5 \times 10^{-4}$	6
ΔM_K	(67)	$\lvert 0.043\,\mathrm{Re}(\kappa^{\mathrm{L}}_{cd} + \kappa^{\mathrm{L}}_{cs}) - 0.015\,\mathrm{Im}\kappa^{\mathrm{L}}_{cs} - \mathrm{Re}(\kappa^{\mathrm{R}*}_{cd}\kappa^{\mathrm{R}}_{cs}) + 0.28\,\mathrm{Im}(\kappa^{\mathrm{R}*}_{cd}\kappa^{\mathrm{R}}_{cs})\rvert \leq 8.5 \times 10^{-4}$	7
ϵ (mixing)	(69)	$\lvert 0.015\,\mathrm{Re}(\kappa^{\mathrm{L}}_{cs} + \kappa^{\mathrm{L}}_{cd}) + 0.043\,\mathrm{Im}\kappa^{\mathrm{L}}_{cs} - 0.28\,\mathrm{Re}(\kappa^{\mathrm{R}*}_{cd}\kappa^{\mathrm{R}}_{cs}) - \mathrm{Im}(\kappa^{\mathrm{R}*}_{cd}\kappa^{\mathrm{R}}_{cs})\rvert \leq 2.5 \times 10^{-6}$	8
ΔM_d	(73)	$-0.031 \leq \mathrm{Re}(\kappa^{\mathrm{L}}_{cb} + \kappa^{\mathrm{L}}_{cd}) + 0.4\,\mathrm{Im}\kappa^{\mathrm{L}}_{cb} \leq 0.003$	9
$\sin(2\beta)$ (mixing)	(77)	$-1.5 \times 10^{-3} \leq 0.4\,\mathrm{Re}(\kappa^{\mathrm{L}}_{cb} + \kappa^{\mathrm{L}}_{cd}) - 0.69\,\mathrm{Im}\kappa^{\mathrm{L}}_{cb} - 0.31\,\mathrm{Im}\kappa^{\mathrm{L}}_{cs} \leq 0.012$	10
ΔM_s	(81)	$-0.014 \leq \mathrm{Re}(\kappa^{\mathrm{L}}_{cs} + \kappa^{\mathrm{L}}_{cb}) + 0.018\,\mathrm{Im}(\kappa^{\mathrm{L}}_{cs} - \kappa^{\mathrm{L}}_{cb}) \leq 0.015$	11
$\sin(2\beta_s)$ (mixing)	(85)	$-0.09 \leq 0.026\,\mathrm{Re}(\kappa^{\mathrm{L}}_{cb} + \kappa^{\mathrm{L}}_{cs}) + \mathrm{Im}(\kappa^{\mathrm{L}}_{cb} - \kappa^{\mathrm{L}}_{cs}) \leq 7 \times 10^{-4}$	12

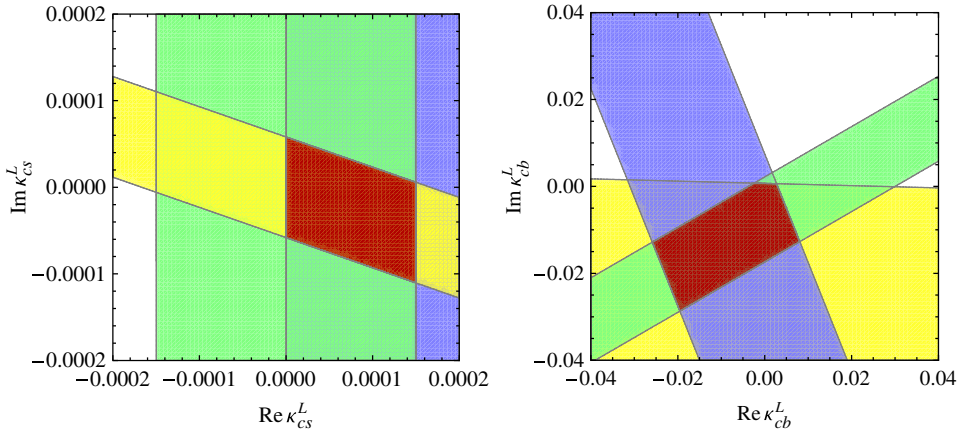

FIG. 1 (color online). Parameter space of the real and imaginary parts of κ^{L}_{cs} and κ^{L}_{cb} subject to the relevant constraints in Table I, under the assumption that only one κ is nonzero at a time. The heavily (blue), medium (green), and lightly (yellow) shaded areas in the left plot satisfy constraints #2, #6, and #8, respectively. The heavily (blue), medium (green), and lightly (yellow) shaded in the right plot satisfy constraints #9, #10, and #12, respectively. The dark (red) region in each plot satisfies all the constraints in it.

and (53) and imposing the constraints in Eqs. (42), (45), and (54). In each of the plots, the very lightly shaded (yellow) band satisfies the ϵ'/ϵ constraint, the lightly shaded (pink) band the ϵ constraint, the medium shaded (green) band the $A_{\Xi\Lambda}$ constraint, the heavily shaded (blue) band the d_n constraint, and the dark (red) region all of the constraints. It is worth noting that there is a significant amount of the parameter space where all of the constraints can be simultaneously satisfied and that the values of $\mathrm{Im}\kappa^{\mathrm{R}}_{cd,cs}$ involved are typically of order a few times 10^{-3} or less. Furthermore, as is obvious from the plots, the neutron-EDM constraint is the most restrictive. Also, interestingly, the allowed region of parameter space easily accommodates an $A_{\Xi\Lambda}$ much larger than the SM prediction, as hinted at by the preliminary measurement by HyperCP [31].

In order to gain some insight into the constraints in Table I and Fig. 2, we have extracted the ranges corresponding to taking only one anomalous coupling at a time to be nonzero (and only for the cases of a purely real or a purely imaginary coupling). They are collected in Table II. This table shows that, in general, the left-handed couplings are much more constrained than the right-handed couplings. Similarly, the imaginary part of the couplings is more tightly constrained than the corresponding real part. The largest deviations allowed by current data appear in the real part of the right-handed couplings, which can be as large as 10% of the corresponding SM couplings.

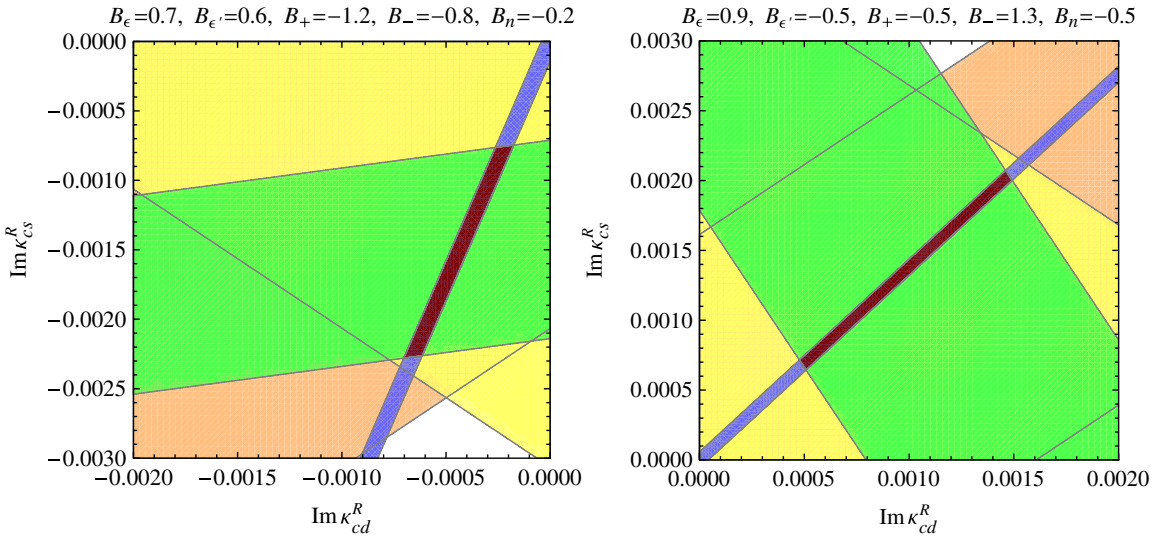

FIG. 2 (color online). Parameter space of $\mathrm{Im}\kappa^{\mathrm{R}}_{cd}$ and $\mathrm{Im}\kappa^{\mathrm{R}}_{cs}$ subject to constraints from the contributions of magnetic-dipole operators to ϵ, ϵ', $A_{\Xi\Lambda}$, and the neutron EDM for two representative sets of $B_{\epsilon,\epsilon',+,-,n}$. The various regions are described in the text.

TABLE II. Constraints on each of the anomalous charm couplings, extracted from Table I and Fig. 2.

$0 \le \mathrm{Re}\kappa^{\mathrm{L}}_{cd} \le 1.5 \times 10^{-4}$	#6	$(\mathrm{Im}\kappa^{\mathrm{L}}_{cd} = 0)$	...
$0 \le \mathrm{Re}\kappa^{\mathrm{L}}_{cs} \le 1.5 \times 10^{-4}$	#2, #6	$-6 \times 10^{-5} \le \mathrm{Im}\kappa^{\mathrm{L}}_{cs} \le 6 \times 10^{-5}$	#8
$-4 \times 10^{-3} \le \mathrm{Re}\kappa^{\mathrm{L}}_{cb} \le 3 \times 10^{-3}$	#9, #10	$-0.02 \le \mathrm{Im}\kappa^{\mathrm{L}}_{cb} \le 7 \times 10^{-4}$	#10, #12
$-0.04 \le \mathrm{Re}\kappa^{\mathrm{R}}_{cd} \le 0.04$	#1	$-2 \times 10^{-3} \le \mathrm{Im}\kappa^{\mathrm{R}}_{cd} \le 2 \times 10^{-3}$	Figure 2
$-0.1 \le \mathrm{Re}\kappa^{\mathrm{R}}_{cs} \le 0$	#2	$-5 \times 10^{-4} \le \mathrm{Im}\kappa^{\mathrm{R}}_{cs} \le 2 \times 10^{-3}$	#4, Fig. 2
$-0.13 \le \mathrm{Re}\kappa^{\mathrm{R}}_{cb} \le 0$	#3	$-5 \times 10^{-4} \le \mathrm{Im}\kappa^{\mathrm{R}}_{cb} \le 0.04$	#4

For specific model building, it is useful to recall that the new physics in the quark-mixing matrices is being parametrized here as the product of the anomalous coupling and the corresponding CKM matrix element, as can be seen in Eqs. (A2) and (A3). The allowed new physics in the left-handed sector is at most of $\mathcal{O}(\lambda^4)$ for the cb coupling and of $\mathcal{O}(\lambda^6)$ for the other two, $\lambda \sim 0.23$ being the usual Cabibbo parameter. This conclusion also implies that current data allow deviations from unitarity in the quark-mixing matrix only at $\mathcal{O}(\lambda^5)$ or higher. On the other hand, new physics affecting right-handed quarks can be of $\mathcal{O}(\lambda^3)$ for cd and cb transitions, and as large as $\mathcal{O}(\lambda)$ for cs transitions. That is to say that the right-handed cs matrix-element is the least constrained.

Perhaps surprisingly, we note that the constraints displayed in Table II are comparable or tighter than existing constraints on anomalous W-boson couplings to the top quark [3]. We can gain more insight into these numbers by interpreting them in the context of left-right (LR) models with mixing of the W_{L} and W_{R} gauge bosons. In these models one predicts $\kappa^{\mathrm{L}} \simeq -\frac{1}{2}\xi^2_W$, where ξ_W is the W_{L}-W_{R} mixing angle. This angle is constrained by $b \to s\gamma$ to be at the 10^{-3} level [40], and so κ^{L} in these models is only allowed at the 10^{-6} level. The additional freedom found in our study arises from the general decoupling between the top and charm anomalous couplings.

For the right-handed anomalous charm couplings, the LR models result in the generic form $\kappa^{\mathrm{R}}_{cD} \simeq (g_{\mathrm{R}}/g_{\mathrm{L}})\xi_W V^{\mathrm{R}}_{cD}/V_{cD}$ for $D = d, s, b$. The first factor, $(g_{\mathrm{R}}/g_{\mathrm{L}})\xi_W$, is allowed to be several times larger than ξ_W [40], whereas the second factor depends on the right-handed mixing matrix, V^{R}. Our bounds in Table II suggest within this context that constraints on right-handed mixing-matrix elements involving charm, V^{R}_{cD}, are not very tight at present, with V^{R}_{cs} being the least constrained one.

Finally, our study also indicates which future measurements provide the most sensitive tests for new physics that can be parametrized with anomalous charm-W couplings. For the CP-violating imaginary parts, the n EDM and the hyperon asymmetry $A_{\Xi\Lambda}$ are the most promising channels for probing right-handed couplings. To probe CP-violating left-handed couplings, more precise measurements of $\sin(2\beta)$ and $\sin(2\beta_s)$ are desired. Constraints on the real parts of the right-handed couplings can be tightened with improved measurements of semileptonic B and D decays.

ACKNOWLEDGMENTS

The work of X. G. H. and J. T. was supported in part by NSC and NCTS. The work of G. V. was supported in part by DOE under Contract No. DE-FG02-01ER41155. We thank David Atwood for useful conversations.

APPENDIX A: INDEPENDENT PARAMETERS IN QUARK-MIXING MATRICES

The parametrization we introduced in Eq. (1) reflects two effective matrices, $K^{\mathrm{L,R}}_{\mathrm{eff}}$, for the charged currents involving left- and right-handed quarks, respectively. In the effective theory under consideration, these 3×3 matrices are complex and nonunitary; the usual unitarity of the CKM matrix is lost. The general 3×3 complex matrix has 18 parameters: 9 magnitudes and 9 phases. Nevertheless, not all the parameters in the matrix describing the left-handed charged current are independent. Of the 9 phases, 5 can be removed by redefinitions of the quark fields. Considering a scenario in which the corrections to the CKM picture in the SM are small, we find it convenient to choose these parameters as

$$K^{\mathrm{L}}_{\mathrm{eff}} = \begin{pmatrix} V_{ud} & V_{us} & V_{ub}e^{i\phi_{ub}} \\ V_{cd}(1+|\kappa^{\mathrm{L}}_{cd}|e^{i\phi^{\mathrm{L}}_{cd}}) & V_{cs}(1+|\kappa^{\mathrm{L}}_{cs}|e^{i\phi^{\mathrm{L}}_{cs}}) & V_{cb}(1+|\kappa^{\mathrm{L}}_{cb}|e^{i\phi^{\mathrm{L}}_{cb}}) \\ V_{td}e^{i\phi_{td}} & V_{ts} & V_{tb} \end{pmatrix}. \tag{A1}$$

More explicitly, four of the five quark phases have been used to remove the phases in V_{ud}, V_{us}, V_{ts}, and V_{tb}. The remaining quark phase has to be used to remove one of the phases in the charm row, and for convenience we choose it to be ϕ_{cd}, thus setting it to zero. Equivalently, only the two relative phases between the three $(K^{\mathrm{L}}_{\mathrm{eff}})_{ci}$ elements are physical. These, plus the phases ϕ_{ub} and ϕ_{td} of V_{ub} and V_{td} which become independent, are the four physical

phases in the general (nonunitary) 3×3 complex matrix. In this study we only allow for three physical phases by requiring that the phases of V_{ub} and V_{td} be related, as in the usual CKM picture.

There are also nine independent real parameters, the magnitudes of each of the elements of $K^{\rm L}_{\rm eff}$. For our study we concentrate on the possibility of new physics in the charm sector, leading us to reduce the number of free parameters that we consider from 9 to 6 by simply setting the other 3 to zero. We choose 3 of the 6 to be the 3 angles that describe the usual CKM matrix and the rest the 3 anomalous couplings that appear explicitly in $K^{\rm L}_{\rm eff}$. We are thus left with

$$K^{\rm L}_{\rm eff} = \begin{pmatrix} 1-\frac{\lambda^2}{2} & \lambda & A\lambda^3(\rho - i\eta) \\ -\lambda(1+|\kappa^{\rm L}_{cd}|) & (1-\frac{\lambda^2}{2})(1+|\kappa^{\rm L}_{cs}|e^{i\phi^{\rm L}_{cs}}) & A\lambda^2(1+|\kappa^{\rm L}_{cb}|e^{i\phi^{\rm L}_{cb}}) \\ A\lambda^3(1-\rho-i\eta) & -A\lambda^2 & 1 \end{pmatrix}, \tag{A2}$$

where, for simplicity of notation, we have included here only the usual terms up to order λ^3 in the Wolfenstein parametrization of the CKM matrix; the complete, unitary CKM matrix should be understood as remaining in Eq. (A2) in the limit $\kappa_{ci} \to 0$ and $\phi_{cj} \to 0$. In this paper we have provided formulas for the relevant observables in terms of these nine parameters. This set of formulas would allow us, in principle, to repeat the global fits for this scenario and constrain the nine parameters. We content ourselves with a less ambitious analysis in which we assume, in accord with observation, that the CKM picture is dominant and deviations are small. We thus use the CKM parameters as extracted from the global fits of CKMfitter [28] as input. The subsequent comparison of this global fit with specific observables then reflects the extent to which deviations from unitarity are allowed by current data. Conservatively, we carry out this comparison at the one-sigma level.

None of the above considerations apply to the right-handed charged current: all the SM field phases are fixed by the removal of five phases in $K^{\rm L}_{\rm eff}$ so that all 18 parameters in the corresponding $K^{\rm R}_{\rm eff}$ are physical. In this study we limit ourselves to 6 of them, which we write as

$$K^{\rm R}_{\rm eff} = \begin{pmatrix} 0 & 0 & 0 \\ -\lambda|\kappa^{\rm R}_{cd}|e^{i\phi^{\rm R}_{cd}} & (1-\frac{\lambda^2}{2})|\kappa^{\rm R}_{cs}|e^{i\phi^{\rm R}_{cs}} & A\lambda^2|\kappa^{\rm R}_{cb}|e^{i\phi^{\rm R}_{cb}} \\ 0 & 0 & 0 \end{pmatrix}. \tag{A3}$$

As pointed out in the conclusion, one needs to keep in mind with this parametrization that the new physics is not just κ_{ij} but its product with V_{ij}, as explicitly seen in Eq. (A3).

APPENDIX B: AMPLITUDES IN UNITARY GAUGE

The loop diagrams that are relevant to some of the processes we consider are displayed in Figs. 3 and 4. In evaluating the diagrams, we use dimensional regularization with a completely anticommuting γ_5 and adopt the unitary gauge, which implies that they contain only fermions and W-bosons. Since the theory with anomalous couplings is not renormalizable, some of the one-loop results are divergent. For these we adopt the prescription to drop the combination $2/(4-D) - \gamma_{\rm E} + \ln(4\pi)$ in the D-dimensional integral, $\gamma_{\rm E}$ being the Euler constant, and retain the accompanying logarithmic, $\ln(\mu/m_W)$, part as well as other finite terms that depend on the mass of the quark in the loop. Moreover, we identify the renormalization scale μ with the scale Λ of the new physics parametrized by the anomalous couplings, $\mu = \Lambda$. In the SM limit ($\kappa^{\rm L,R} = 0$), after the unitarity relation $V^*_{ud'}V_{ud} + V^*_{cd'}V_{cd} + V^*_{td'}V_{td} = 0$ is imposed, our results are finite and reproduce those obtained in the literature in R_ξ gauges [33].

We will present the details of our calculation elsewhere [41]. Here we provide the resulting effective Hamiltonians relevant to the loop-induced processes dealt with in this paper.

The effective Hamiltonians for electromagnetic and chromomagnetic dipole operators involving down-type quarks d and $d' \neq d$ are derived from the four diagrams in Fig. 3 with up-type quarks q in the loops and can be expressed as

$$\mathcal{H}_{d\to d'\gamma} = \frac{-eG_{\rm F}}{4\sqrt{2}\pi^2} \sum_{q=u,c,t} \bar{d}'\sigma_{\mu\nu}(F^q_{\rm L}P_{\rm L} + F^q_{\rm R}P_{\rm R})dF^{\mu\nu}, \tag{B1}$$

FIG. 3. Diagrams contributing to amplitudes for $d \to d'\mathcal{V}^*$, with $\mathcal{V}$ being a neutral gauge boson. In all diagram figures, straight lines denote fermions and the loops contain W bosons besides fermions.

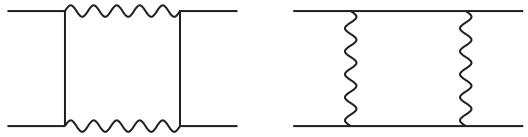

(a) (b)

FIG. 4. Box diagrams contributing to amplitudes for (a) $d\bar{d}' \to \ell^+\ell^-$ or $\bar{\nu}\nu$ and (a,b) $d\bar{d}' \to d\bar{d}'$.

$$\mathcal{H}_{d\to d'g} = \frac{-g_s G_F}{4\sqrt{2}\pi^2} \sum_{q=u,c,t} \bar{d}'\sigma_{\mu\nu}(G_L^q P_L + G_R^q P_R) t_a d G_a^{\mu\nu}, \tag{B2}$$

where $\sigma^{\mu\nu} = \frac{i}{2}[\gamma^\mu, \gamma^\nu]$,

$$\begin{aligned} F_L^q &= (\lambda_q^L m_{d'} + \lambda_q^R m_d) F_0^{SM}(x_q) \\ &\quad + \lambda_q (1 + \kappa_{qd}^L)\kappa_{qd'}^{R*} m_q F_0(x_q), \\ F_R^q &= (\lambda_q^L m_d + \lambda_q^R m_{d'}) F_0^{SM}(x_q) \\ &\quad + \lambda_q (1 + \kappa_{qd'}^{L*})\kappa_{qd}^R m_q F_0(x_q), \end{aligned} \tag{B3}$$

$$\begin{aligned} G_L^q &= (\lambda_q^L m_{d'} + \lambda_q^R m_d) G_0^{SM}(x_q) \\ &\quad + \lambda_q (1 + \kappa_{qd}^L)\kappa_{qd'}^{R*} m_q G_0(x_q), \\ G_R^q &= (\lambda_q^L m_d + \lambda_q^R m_{d'}) G_0^{SM}(x_q) \\ &\quad + \lambda_q (1 + \kappa_{qd'}^{L*})\kappa_{qd}^R m_q G_0(x_q), \end{aligned} \tag{B4}$$

with

$$\begin{aligned} &\lambda_q = V_{qd'}^* V_{qd}, \qquad \lambda_q^L = \lambda_q (1 + \kappa_{qd'}^{L*})(1 + \kappa_{qd}^L), \\ &\lambda_q^R = \lambda_q \kappa_{qd'}^{R*} \kappa_{qd}^R, \qquad x_f = \frac{\bar{m}_f^2(m_f)}{m_W^2}, \end{aligned} \tag{B5}$$

$$\begin{aligned} F_0^{SM}(x) &= \frac{-7x + 5x^2 + 8x^3}{24(1-x)^3} - \frac{2x^2 - 3x^3}{4(1-x)^4} \ln x, \\ F_0(x) &= \frac{-20 + 31x - 5x^2}{12(1-x)^2} - \frac{2x - 3x^2}{2(1-x)^3} \ln x, \end{aligned} \tag{B6}$$

$$\begin{aligned} G_0^{SM}(x) &= \frac{-2x - 5x^2 + x^3}{8(1-x)^3} - \frac{3x^2 \ln x}{4(1-x)^4}, \\ G_0(x) &= \frac{-4 - x - x^2}{4(1-x)^2} - \frac{3x \ln x}{2(1-x)^3}. \end{aligned} \tag{B7}$$

We note that the loop calculation for these operators yields finite results. We also note that different notations, $D_0' = -2F_0^{SM}$, $E_0' = -2G_0^{SM}$, $\tilde{F} = F_0$, and $\tilde{G} = G_0$, are sometimes used in the literature [21,22].

The process $d\bar{d}' \to \nu\bar{\nu}$ receives contributions from all the diagrams in Fig. 3 via $d\bar{d}' \to Z^* \to \nu\bar{\nu}$ and from the box diagram in Fig. 4(a), the loop fermions in the latter being an up-type quark and a lepton. After summing over $q = u, c, t$ and imposing the unitarity condition $\lambda_u + \lambda_c + \lambda_t = 0$, we find the effective Hamiltonian

$$\mathcal{H}_{d\bar{d}'\to\nu\bar{\nu}} = \mathcal{H}^{SM}_{d\bar{d}'\to\nu\bar{\nu}} + \mathcal{H}^{\kappa}_{d\bar{d}'\to\nu\bar{\nu}}, \tag{B8}$$

where

$$\mathcal{H}^{SM}_{d\bar{d}'\to\nu\bar{\nu}} = \frac{\alpha G_F}{\sqrt{8}\pi \sin^2\theta_W} \sum_q 4\lambda_q X_0(x_q) \bar{d}'\gamma^\sigma P_L d\bar{\nu}\gamma_\sigma P_L \nu, \tag{B9}$$

$$\begin{aligned} \mathcal{H}^{\kappa}_{d\bar{d}'\to\nu\bar{\nu}} &= \frac{\alpha G_F}{\sqrt{8}\pi \sin^2\theta_W} \sum_q (\lambda_q^L - \lambda_q)\left(-3\ln\frac{\Lambda}{m_W} + 4X_0(x_q)\right) \\ &\quad \times \bar{d}'\gamma^\sigma P_L d\bar{\nu}\gamma_\sigma P_L \nu + \frac{\alpha G_F}{\sqrt{8}\pi \sin^2\theta_W} \\ &\quad \times \sum_q \lambda_q^R \left[(4x_q - 3)\ln\frac{\Lambda}{m_W} + \tilde{X}(x_q)\right] \\ &\quad \times \bar{d}'\gamma^\sigma P_R d\bar{\nu}\gamma_\sigma P_L \nu, \end{aligned} \tag{B10}$$

with

$$\begin{aligned} X_0(x) &= \frac{x(x+2)}{8(x-1)} + \frac{3x(x-2)}{8(x-1)^2} \ln x, \\ \tilde{X}(x) &= 2x - \frac{5x - 2x^2}{1-x} \ln x - 4X_0(x). \end{aligned} \tag{B11}$$

In the expressions for $\mathcal{H}_{d\bar{d}'\to\nu\bar{\nu}}$ above, we have neglected the dependence on the mass of the loop lepton in the box diagram, but it is possible to generalize the formulas to include the dependence on tau-lepton mass [41].

The amplitude for $d\bar{d}' \to \ell^+\ell^-$ gets contributions from all the diagrams in Fig. 3 via $d\bar{d}' \to (\gamma^*, Z^*) \to \ell^+\ell^-$ and the diagram in Fig. 4(a), the loop fermions in the latter being an up-type quark and a neutrino. The resulting effective Hamiltonian is

$$\mathcal{H}_{d\bar{d}'\to\ell^+\ell^-} = \mathcal{H}^{SM}_{d\bar{d}'\to\ell^+\ell^-} + \mathcal{H}^{\kappa}_{d\bar{d}'\to\ell^+\ell^-}, \tag{B12}$$

where

$$\begin{aligned} \mathcal{H}^{SM}_{d\bar{d}'\to\ell^+\ell^-} &= \frac{\alpha G_F}{\sqrt{8}\pi} \sum_q 4\lambda_q \left(\frac{-Y_0(x_q)}{\sin^2\theta_W} \bar{d}'\gamma^\sigma P_L d\bar{\ell}\gamma_\sigma P_L \ell \right. \\ &\quad \left. + 2Z_0(x_q)\bar{d}'\gamma^\sigma P_L d\bar{\ell}\gamma_\sigma \ell\right), \end{aligned} \tag{B13}$$

$$\mathcal{H}^{\kappa}_{d\bar{d}'\to\ell^+\ell^-} = \frac{\alpha G_F}{\sqrt{8}\pi}\sum_q(\lambda_q^L-\lambda_q)\Big[\Big(3\ln\frac{\Lambda}{m_W}-4Y_0(x_q)\Big)\times\frac{\bar{d}'\gamma^\sigma P_L d\bar{\ell}\gamma_\sigma P_L\ell}{\sin^2\theta_W}+\Big(-\frac{16}{3}\ln\frac{\Lambda}{m_W}+8Z_0(x_q)\Big)\bar{d}'\gamma^\sigma P_L d\bar{\ell}\gamma_\sigma\ell\Big]+\frac{\alpha G_F}{\sqrt{8}\pi}\sum_q\lambda_q^R\times\Big\{\Big[(3-4x_q)\ln\frac{\Lambda}{m_W}+\tilde{Y}(x_q)\Big]\times\frac{\bar{d}'\gamma^\sigma P_R d\bar{\ell}\gamma_\sigma P_L\ell}{\sin^2\theta_W}+\Big[\Big(8x_q-\frac{16}{3}\Big)\ln\frac{\Lambda}{m_W}+\tilde{Z}(x_q)\Big]\bar{d}'\gamma^\sigma P_R d\bar{\ell}\gamma_\sigma\ell\Big\}, \tag{B14}$$

with

$$Y_0(x)=\frac{x(x-4)}{8(x-1)}+\frac{3x^2}{8(x-1)^2}\ln x,$$
$$Z_0(x)=\frac{18x^4-163x^3+259x^2-108x}{144(x-1)^3}+\frac{24x^4-6x^3-63x^2+50x-8}{72(x-1)^2}\ln x, \tag{B15}$$

$$\tilde{Y}(x)=-2x+\frac{5x-2x^2}{1-x}\ln x+4Y_0(x),$$
$$\tilde{Z}(x)=2x-4x\ln x+8Z_0(x). \tag{B16}$$

In $\mathcal{H}^{SM,\kappa}_{d\bar{d}'\to\ell^+\ell^-}$ above, we have not displayed terms contributed by the magnetic ($\sigma^{\mu\nu}$) parts of the $d\bar{d}'\to(\gamma^*,Z^*)$ amplitudes for convenience, but they can be found in Ref. [41] and do not contribute to the decay $K_L\to\mu^+\mu^-$, which we consider. We note that the SM results in Eqs. (B9) and (B13) are in agreement with those found in the literature [21,33].

From the two box diagrams in Fig. 4 with quarks d and d' in the external legs and quarks q and q' in the loops, we derive the effective Hamiltonian

$$\mathcal{H}_{d\bar{d}'\to\bar{d}d'}=\mathcal{H}^{SM}_{d\bar{d}'\to\bar{d}d'}+\mathcal{H}^{\kappa}_{d\bar{d}'\to\bar{d}d'}, \tag{B17}$$

where

$$\mathcal{H}^{SM}_{d\bar{d}'\to\bar{d}d'}=\frac{G_F^2m_W^2}{4\pi^2}(\lambda_c^2S_0(x_c)+\lambda_t^2S_0(x_t)+2\lambda_c\lambda_tS_0(x_c,x_t))\bar{d}'\gamma^\alpha P_L d\bar{d}'\gamma_\alpha P_L d, \tag{B18}$$

$$\mathcal{H}^{\kappa}_{d\bar{d}'\to\bar{d}d'}=\frac{G_F^2m_W^2}{16\pi^2}\sum_{q,q'}(\lambda_q^L\lambda_{q'}^L-\lambda_q\lambda_{q'})\Big[(6-2x_q)\ln\frac{\Lambda^2}{m_W^2}-\mathcal{B}_1(x_q,x_{q'})\Big]\bar{d}'\gamma^\alpha P_L d\bar{d}'\gamma_\alpha P_L d+\frac{G_F^2m_W^2}{4\pi^2}\times\sum_{q,q'}\lambda_q\lambda_{q'}^R\Big[(6-x_q-x_{q'})\ln\frac{\Lambda^2}{m_W^2}-\mathcal{B}_2(x_q,x_{q'})\Big]\times\bar{d}'\gamma^\alpha P_L d\bar{d}'\gamma_\alpha P_R d+\frac{G_F^2m_W^2}{4\pi^2}\sum_{q,q'}\lambda_q\lambda_{q'}\sqrt{x_qx_{q'}}\times\Big(-\ln\frac{\Lambda^2}{m_W^2}-\mathcal{B}_3(x_q,x_{q'})\Big)(\kappa^R_{qd}\kappa^R_{q'd}\bar{d}'P_R d\bar{d}'P_R d+\kappa^{R*}_{qd'}\kappa^{R*}_{q'd'}\bar{d}'P_L d\bar{d}'P_L d), \tag{B19}$$

with

$$S_0(x,y)=\frac{-3xy}{4(1-x)(1-y)}-\frac{xy(4-8x+x^2)\ln x}{4(y-x)(1-x)^2}-\frac{xy(4-8y+y^2)\ln y}{4(x-y)(1-y)^2}, \tag{B20}$$

$$\mathcal{B}_1(x,y)=\frac{3}{2}(x+y)+\frac{3(x+y-xy)}{(1-x)(1-y)}+\frac{(4x^2-8x^3+x^4)\ln x}{(y-x)(1-x)^2}+\frac{(4y^2-8y^3+y^4)\ln y}{(x-y)(1-y)^2},$$
$$\mathcal{B}_2(x,y)=\frac{3}{2}(x+y)-\frac{9(x+y-xy)}{(1-x)(1-y)}+\frac{(4-x)^2x^2\ln x}{(y-x)(1-x)^2}+\frac{(4-y)^2y^2\ln y}{(x-y)(1-y)^2}, \tag{B21}$$
$$\mathcal{B}_3(x,y)=\frac{xy-x-y-2}{(1-x)(1-y)}+\frac{(4x-2x^2+x^3)\ln x}{(y-x)(1-x)^2}+\frac{(4y-2y^2+y^3)\ln y}{(x-y)(1-y)^2},$$

and $S_0(x)=\lim_{y\to x}S_0(x,y)$. The expression for $\mathcal{H}^{SM}_{d\bar{d}'\to\bar{d}d'}$ agrees with that in the literature [21,33].

APPENDIX C: MATRIX ELEMENTS AND PARAMETERS

The matrix elements used in estimating the amplitudes for $\bar{B}\to J/\psi\bar{K}$, $\eta_c\bar{K}$ are

$$\langle \psi|\bar{c}_m\gamma^\mu c_n|0\rangle = \frac{\delta_{mn}}{N_c} f_\psi m_\psi \varepsilon^\mu, \qquad \langle \bar{K}^0(q)|\bar{s}_m b_n|\bar{B}^0(p)\rangle = \frac{\delta_{mn}}{N_c}\frac{p^2-q^2}{m_b-m_s}F_0^{BK},$$
$$\langle \bar{K}^0(q)|\bar{s}_m\gamma_\mu b_n|\bar{B}^0(p)\rangle = \frac{\delta_{mn}}{N_c}\left[(p+q)^\mu F_1^{BK} + \frac{(p-q)^\mu}{(p-q)^2}(m_B^2-m_K^2)(F_0^{BK}-F_1^{BK})\right], \tag{C1}$$
$$\langle \eta_c|\bar{c}_m\gamma^\mu\gamma_5 c_n|0\rangle = \frac{\delta_{mn}}{N_c} i f_{\eta_c} p_{\eta_c}^\mu, \qquad \langle \eta_c|\bar{c}_m\gamma_5 c_n|0\rangle = \frac{\delta_{mn}}{N_c}\frac{i f_{\eta_c} m_{\eta_c}^2}{2m_c},$$

where $N_c = 3$ is the number of colors and m and n are color indices. The decay constants above are $f_\psi = 416$ MeV extracted from $\Gamma(J/\psi \to e^+e^-)$ data [13] and $f_{\eta_c} = 420$ MeV calculated in Ref. [42]. The form factors $F_{0,1}^{BK}$ are functions of $(p-q)^2$, with $F_0^{BK}(m_{\eta_c}^2) = 0.45$ and $F_1^{BK}(m_\psi^2) = 0.65$ from Ref. [43]. For meson masses, we use the values in Ref. [13].

The K, B_d, and B_s decay-constants are [13,28]

$$f_K = 155.5 \pm 0.8, \qquad f_{B_d} = 191 \pm 15, \qquad f_{B_s} = 228 \pm 17, \tag{C2}$$

all in units of MeV. All of the following parameter values are obtained from Ref. [28], the experimental and theoretical errors given therein having been combined in quadrature. The QCD-correction factors in the K- and $B_{d,s}$-mixing amplitudes are [21,28,44].

$$\eta_{cc} = 1.46 \pm 0.22, \qquad \eta_B = 0.551 \pm 0.007. \tag{C3}$$

The bag parameters used in the K-mixing amplitude are defined by

$$\langle K^0|\bar{d}\gamma^\alpha P_L s\bar{d}\gamma_\alpha P_L s|\bar{K}^0\rangle = \frac{2}{3} f_K^2 m_K^2 B_K,$$
$$\langle K^0|\bar{d}\gamma^\alpha P_L s\bar{d}\gamma_\alpha P_R s|\bar{K}^0\rangle = \frac{-f_K^2 m_K^4 B_K}{3(m_d+m_s)^2}, \tag{C4}$$

and similarly for $B_{B_{d,s}}$ in the $B_{d,s}$-mixing cases, where [28]

$$B_K = 0.72 \pm 0.04, \qquad B_{B_d} = 1.17 \pm 0.08, \qquad B_{B_s} = 1.23 \pm 0.06. \tag{C5}$$

The charm and top masses used in the loop functions are [28,45]

$$\bar{m}_c(m_c) = 1.29 \pm 0.04, \qquad \bar{m}_t(m_t) = 165 \pm 1, \tag{C6}$$

both in units of GeV. For the CKM parameters, we adopt in the Wolfenstein parametrization the central values [28]

$$A = 0.8116, \qquad \lambda = 0.225\,21, \qquad \bar{\rho} = 0.139, \qquad \bar{\eta} = 0.341. \tag{C7}$$

In our numerical estimates, we use only the central values of the parameters above, as their errors being no more than 20% are within the intrinsic uncertainty of our analysis.

[1] W. Buchmuller and D. Wyler, Nucl. Phys. **B268**, 621 (1986).

[2] R. D. Peccei and X. Zhang, Nucl. Phys. **B337**, 269 (1990); R. D. Peccei, S. Peris, and X. Zhang, Nucl. Phys. **B349**, 305 (1991).

[3] K. Fujikawa and A. Yamada, Phys. Rev. D **49**, 5890 (1994); F. Larios, M. A. Perez, and C. P. Yuan, Phys. Lett. B **457**, 334 (1999); G. Burdman, M. C. Gonzalez-Garcia, and S. F. Novaes, Phys. Rev. D **61**, 114016 (2000); B. Grzadkowski and M. Misiak, Phys. Rev. D **78**, 077501 (2008); J. P. Lee and K. Y. Lee, Phys. Rev. D **78**, 056004 (2008).

[4] D. O. Carlson, E. Malkawi, and C. P. Yuan, Phys. Lett. B **337**, 145 (1994); E. Malkawi and C. P. Yuan, Phys. Rev. D **50**, 4462 (1994).

[5] A. L. Kagan, Phys. Rev. D **51**, 6196 (1995); G. Colangelo, G. Isidori, and J. Portoles, Phys. Lett. B **470**, 134 (1999); G. D'Ambrosio, G. Isidori, and G. Martinelli, Phys. Lett. B **480**, 164 (2000); J. Tandean and G. Valencia, Phys. Rev. D **62**, 116007 (2000); D. N. Gao, Phys. Rev. D **67**, 074028 (2003); F. Mescia, C. Smith, and S. Trine, J. High Energy Phys. 08 (2006) 088.

[6] A. J. Buras, G. Colangelo, G. Isidori, A. Romanino, and L. Silvestrini, Nucl. Phys. **B566**, 3 (2000).

[7] G. Ecker, W. Grimus, and H. Neufeld, Nucl. Phys. **B229**, 421 (1983).

[8] X. G. He, B. H. J. McKellar, and S. Pakvasa, Int. J. Mod. Phys. A **4**, 5011 (1989); **6**, 1063(E) (1991); Phys. Lett. B **254**, 231 (1991).

[9] J. S. M. Ginges and V. V. Flambaum, Phys. Rep. **397**, 63 (2004).

[10] C. Dib, A. Faessler, T. Gutsche, S. Kovalenko, J. Kuckei,

V. E. Lyubovitskij, and K. Pumsa-ard, J. Phys. G **32**, 547 (2006), references therein.
[11] H. Georgi, Annu. Rev. Nucl. Part. Sci. **43**, 209 (1993).
[12] X. G. He and G. Valencia, Phys. Rev. D**70**, 053003 (2004); X. G. He, G. Valencia, and Y. Wang, Phys. Rev. D **70**, 113011 (2004).
[13] C. Amsler *et al.* (Particle Data Group), Phys. Lett. B **667**, 1 (2008).
[14] S. Stone, arXiv:0806.3921; J. P. Alexander (CLEO Collaboration), Phys. Rev. D **79**, 052001 (2009).
[15] B. A. Dobrescu and A. S. Kronfeld, Phys. Rev. Lett. **100**, 241802 (2008); A. S. Kronfeld, Proc. Sci., LATTICE2008 (2008) 282.
[16] S. Narison, Phys. Lett. B **668**, 308 (2008).
[17] R. Kowalewski and T. Mannel, in Ref. [13].
[18] N. Isgur and M. B. Wise, Phys. Lett. B **232**, 113 (1989); A. V. Manohar and M. B. Wise, *Heavy Quark Physics* (Cambridge University Press, Cambridge, 2000).
[19] Heavy Flavor Averaging Group, http://www.slac.stanford.edu/xorg/hfag.
[20] Y. Nir and H. R. Quinn, Annu. Rev. Nucl. Part. Sci. **42**, 211 (1992).
[21] G. Buchalla, A. J. Buras, and M. E. Lautenbacher, Rev. Mod. Phys. **68**, 1125 (1996).
[22] P. L. Cho and M. Misiak, Phys. Rev. D **49**, 5894 (1994).
[23] M. Bauer, B. Stech, and M. Wirbel, Z. Phys. C **34**, 103 (1987); A. Ali and C. Greub, Phys. Rev. D **57**, 2996 (1998); H. Y. Cheng and B. Tseng, Phys. Rev. D **58**, 094005 (1998); A. Ali, G. Kramer, and C. D. Lu, Phys. Rev. D **58**, 094009 (1998).
[24] X. G. He and G. Valencia, Phys. Rev. D **61**, 075003 (2000).
[25] J. F. Donoghue and B. R. Holstein, Phys. Rev. D **32**, 1152 (1985); X. G. He and G. Valencia, Phys. Rev. D **52**, 5257 (1995).
[26] X. G. He, H. Murayama, S. Pakvasa, and G. Valencia, Phys. Rev. D **61**, 071701 (2000).
[27] J. Tandean, Phys. Rev. D **69**, 076008 (2004).
[28] CKMfitter, http://ckmfitter.in2p3.fr.
[29] J. O. Eeg, K. Kumericki, and I. Picek, Phys. Lett. B **669**, 150 (2008); A. J. Buras and D. Guadagnoli, Phys. Rev. D **79**, 053010 (2009).
[30] J. F. Donoghue, X. G. He, and S. Pakvasa, Phys. Rev. D **34**, 833 (1986); X. G. He, H. Steger, and G. Valencia, Phys. Lett. B **272**, 411 (1991); N. G. Deshpande, X. G. He, and S. Pakvasa, *ibid.* **326**, 307 (1994); J. Tandean and G. Valencia, Phys. Rev. D **67**, 056001 (2003).
[31] C. Materniak (HyperCP Collaboration), *Eighth International Conference on Hyperons, Charm and Beauty Hadrons, 2008, Columbia, South Carolina*.
[32] L. Pondrom *et al.*, Phys. Rev. D **23**, 814 (1981).
[33] T. Inami and C. S. Lim, Prog. Theor. Phys. **65**, 297 (1981); **65**, 1772(E) (1981).
[34] A. J. Buras, M. Gorbahn, U. Haisch, and U. Nierste, J. High Energy Phys. 11 (2006) 002; F. Mescia and C. Smith, Phys. Rev. D **76**, 034017 (2007); A. J. Buras, F. Schwab, and S. Uhlig, Rev. Mod. Phys. **80**, 965 (2008); J. Brod and M. Gorbahn, Phys. Rev. D **78**, 034006 (2008).
[35] A. V. Artamonov *et al.* (E949 Collaboration), Phys. Rev. Lett. **101**, 191802 (2008).
[36] M. Gorbahn and U. Haisch, Phys. Rev. Lett. **97**, 122002 (2006).
[37] L. Littenberg and G. Valencia, in Ref. [13].
[38] A. Abd El-Hady and G. Valencia, Phys. Lett. B **414**, 173 (1997).
[39] D. Chang, X. G. He, and S. Pakvasa, Phys. Rev. Lett. **74**, 3927 (1995); A. Masiero and H. Murayama, Phys. Rev. Lett. **83**, 907 (1999).
[40] P. Langacker and S. Uma Sankar, Phys. Rev. D **40**, 1569 (1989); X. G. He and G. Valencia, Phys. Rev. D **66**, 013004 (2002); **66**, 079901(E) (2002).
[41] X. G. He, J. Tandean, and G. Valencia (unpublished).
[42] D. S. Hwang and G. H. Kim, Z. Phys. C **76**, 107 (1997).
[43] H. Y. Cheng, C. K. Chua, and C. W. Hwang, Phys. Rev. D **69**, 074025 (2004).
[44] S. Herrlich and U. Nierste, Nucl. Phys. **B419**, 292 (1994); J. H. Kuhn, M. Steinhauser, and C. Sturm, Nucl. Phys. **B778**, 192 (2007).
[45] I. Allison *et al.* (HPQCD Collaboration), Phys. Rev. D **78**, 054513 (2008); M. Steinhauser, arXiv:0809.1925.